Ion bombardment of multi-wall carbon nanotubes: role of the tube axis alignment

Francesca Ripanti

francesca.ripanti@uniroma1.it

CYGNUS 2019

Seventh workshop on directional dark matter searches

10 - 12 July 2019 - Roma

Istituto Nazionale di Fisica Nucleare
Sezione di Roma

SAPIENZA
Università di Roma

Directional detection in carbon nanotubes

basic idea: study the properties of carbon nanotubes (CNTs) as suitable material for dark matter particle detection

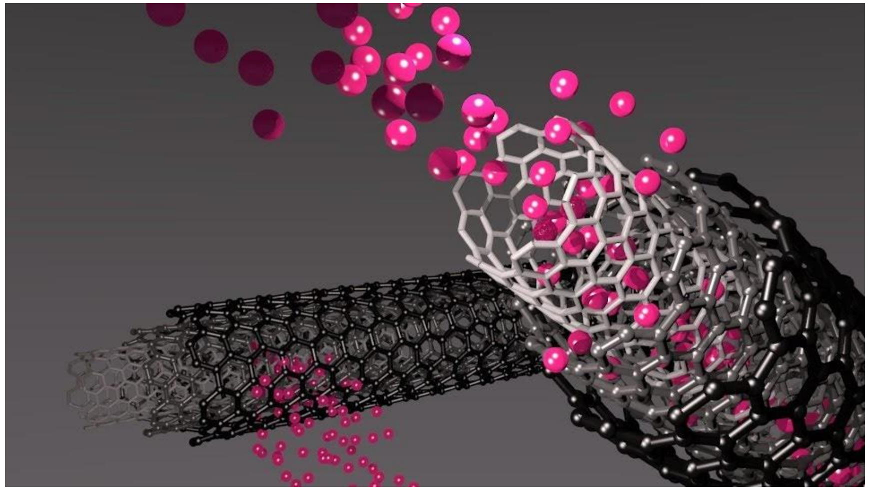

two different experimental challenges:

1. mimic dark matter weakly interacting particles (WIMPs) with Ar^+ ion and analyze the anisotropic response (channeling)

2. careful characterization of the CNT arrays:
   - electronic and structural properties of the detector material
   - comparison with computation results

- ✓ microscopy: morphology & dimensions
- ✓ X-ray photoemission spectroscopy: surface characterization & electronic properties
- ✓ Raman spectroscopy: structural conformations, local analysis, bulk measurements!

MWCNT growth and characterization

Chemical Vapor Deposition
@University of Mons (BE)

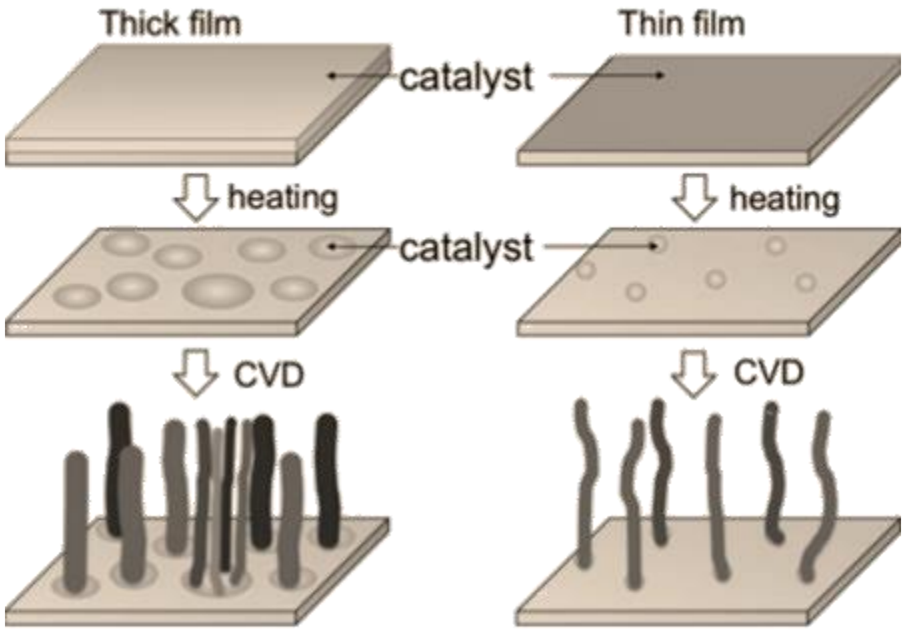

Scanning Electron Microscopy
@CNIS, Sapienza

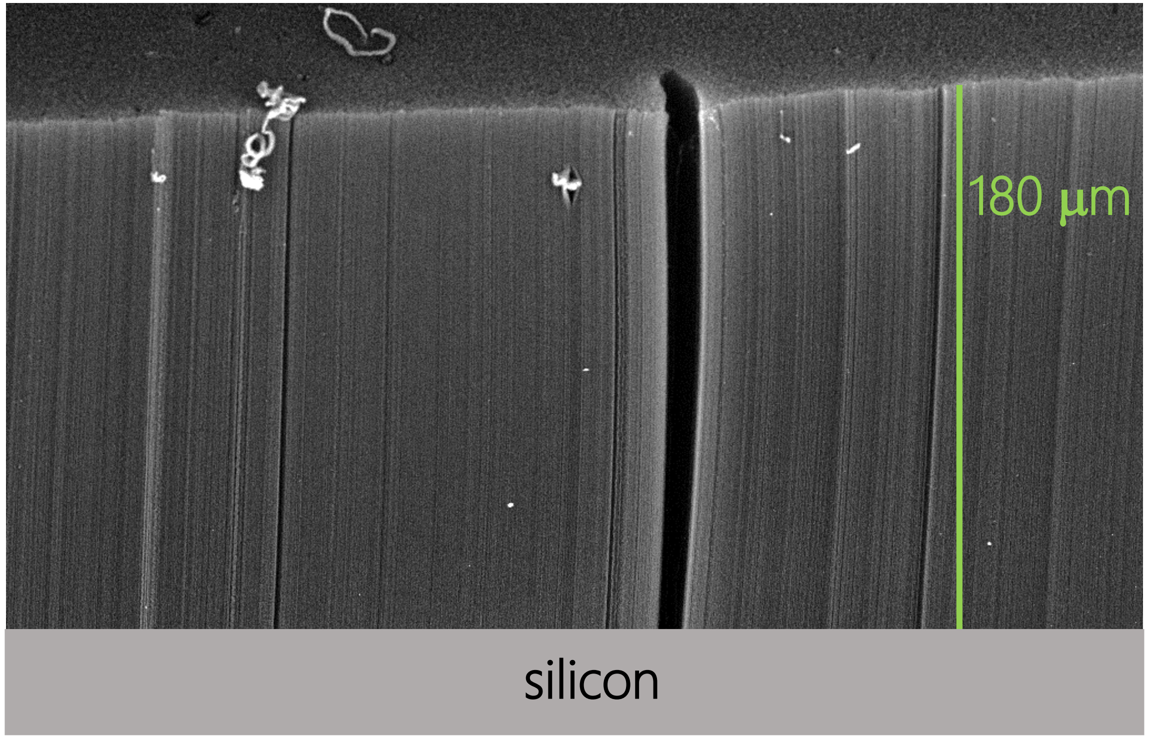

highly aligned MWCNTs

- ✓ very high aspect ratio!
- ✓ height ~ 180 μm
- ✓ diameter ~ 20 nm (~ 25 concentric cylinders each tube!)
- ✓ density ~ $4 \cdot 10^{10}$ tubes/cm^2

Ion bombardment

principal aim: study the directional response of a clearly anisotropic system (carbon nanotubes array)

experimental strategy

two different geometries for ion bombardment:

- TOP bombardment: Ar^+ ions "look" empty spaces
- LAT bombardment: do Ar^+ ions penetrate inside CNT forest?

two different geometries also for collecting signal (either from the top and from the side)

↓

explore all the possible configurations to detect all the possible anisotropy effects

parallel to the CNT axes
TOP bombardment

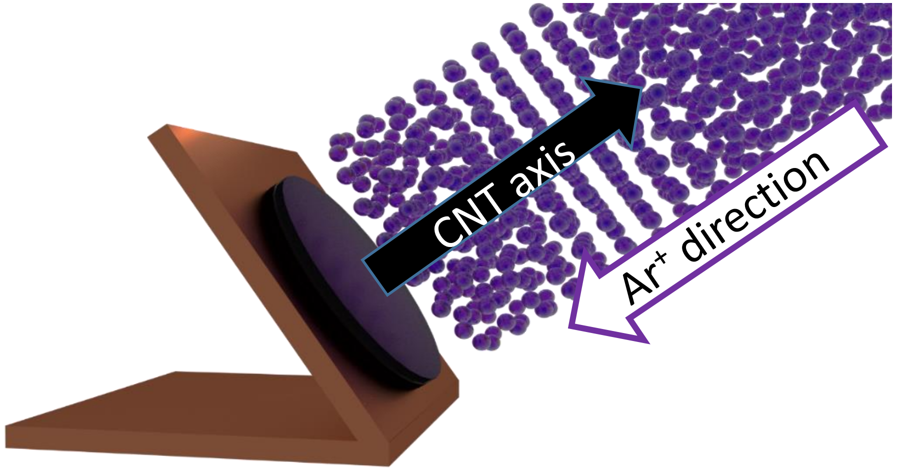

perpendicular to the CNT axes
LAT bombardment

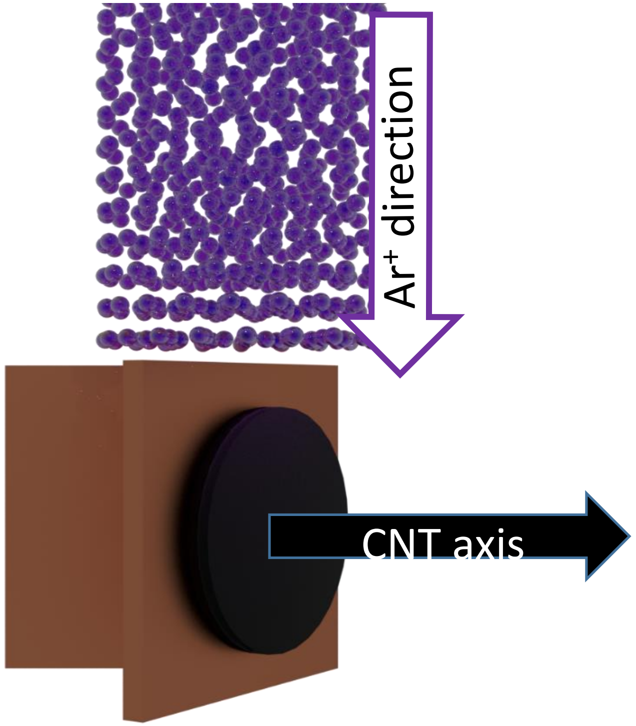

Ar^+ ion bombardment (5keV) produces different spectroscopic response (associated to the carbon damage)

Experimental techniques: XPS

based on the photoelectric effect, i.e., emission of electron following excitation of core level electrons by photons

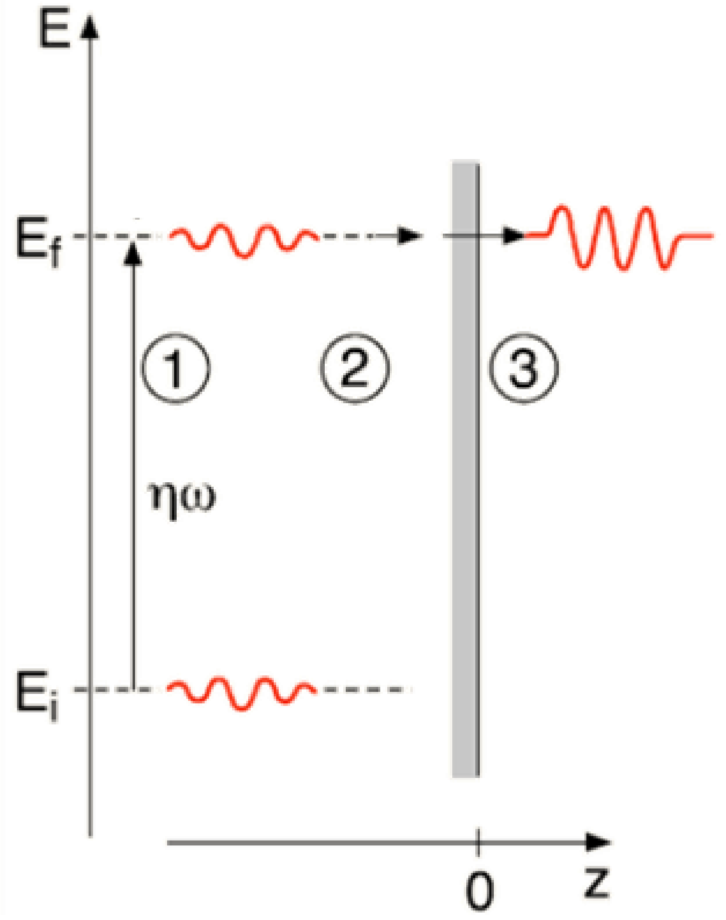

three step model:

1. photon absorption and ionization
2. creation of photoelectron
3. transmission through the surface

Experimental techniques: XPS

based on the photoelectric effect, i.e., emission of electron following excitation of core level electrons by photons

- X-ray monochromatic radiation
- high vacuum chamber
- surface sensitivity
- electronic properties of the system (chemical bonds)

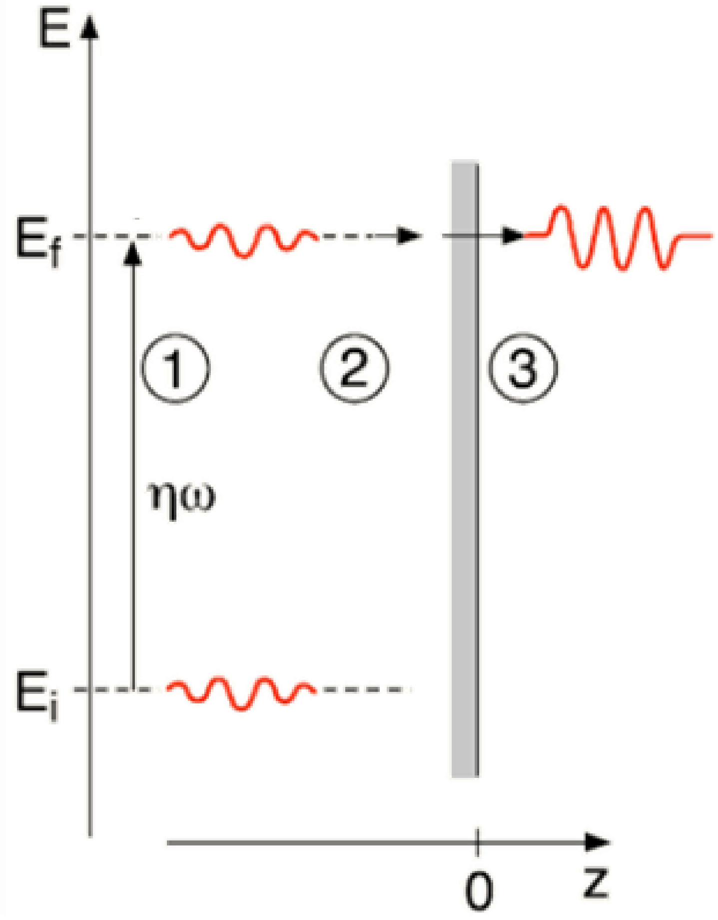

three step model:

1. photon absorption and ionization
2. creation of photoelectron
3. transmission through the surface

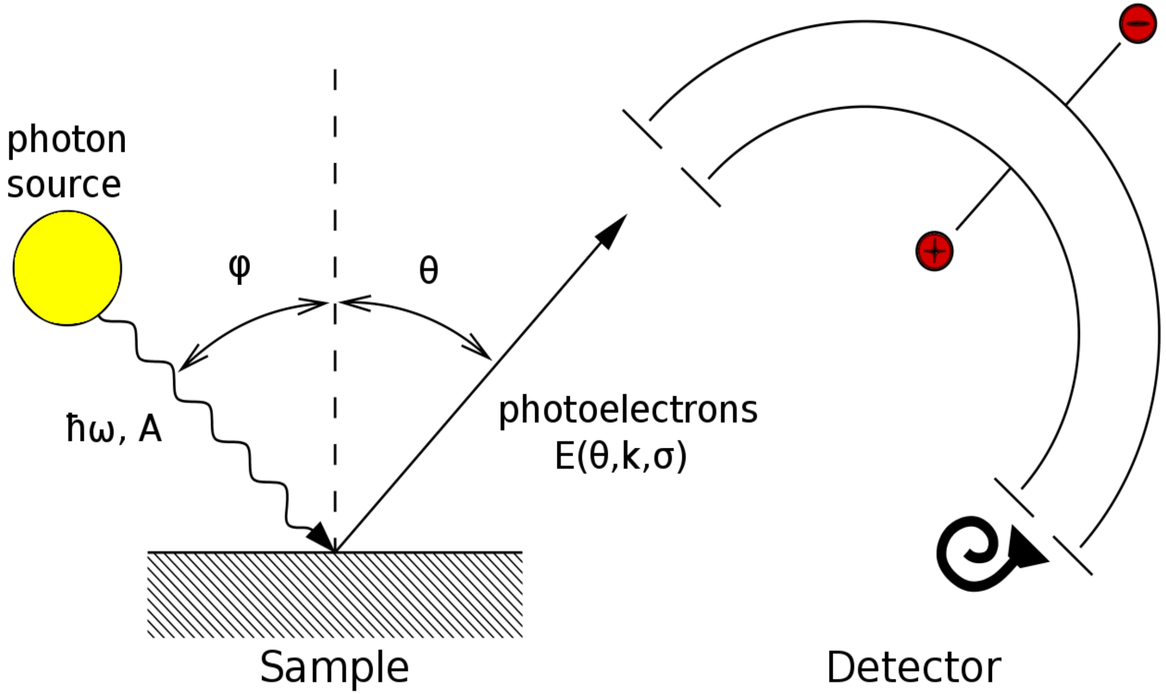

Experimental techniques: Raman spectroscopy

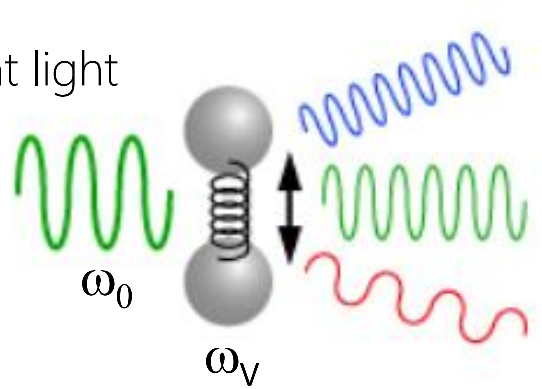

Raman effect: inelastic light scattering

- ✓ vibrational modes $\longleftrightarrow$ chemical bonds
- ✓ structural configuration
- ✓ information on the local 'environment'
- ✓ not only surface!
- ✓ possibility of penetration below the surface

Experimental techniques: Raman spectroscopy

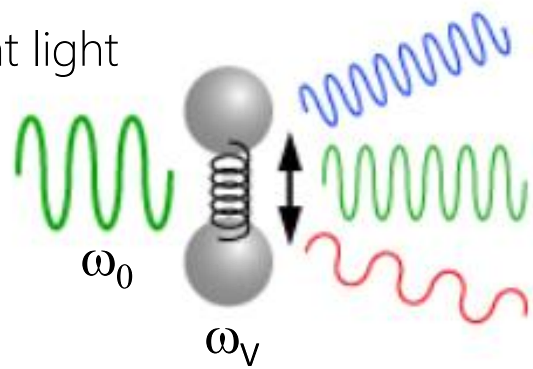

Raman effect: inelastic light scattering

- ✓ vibrational modes ⟷ chemical bonds
- ✓ structural configuration
- ✓ information on the local 'environment'
- ✓ not only surface!
- ✓ possibility of penetration below the surface

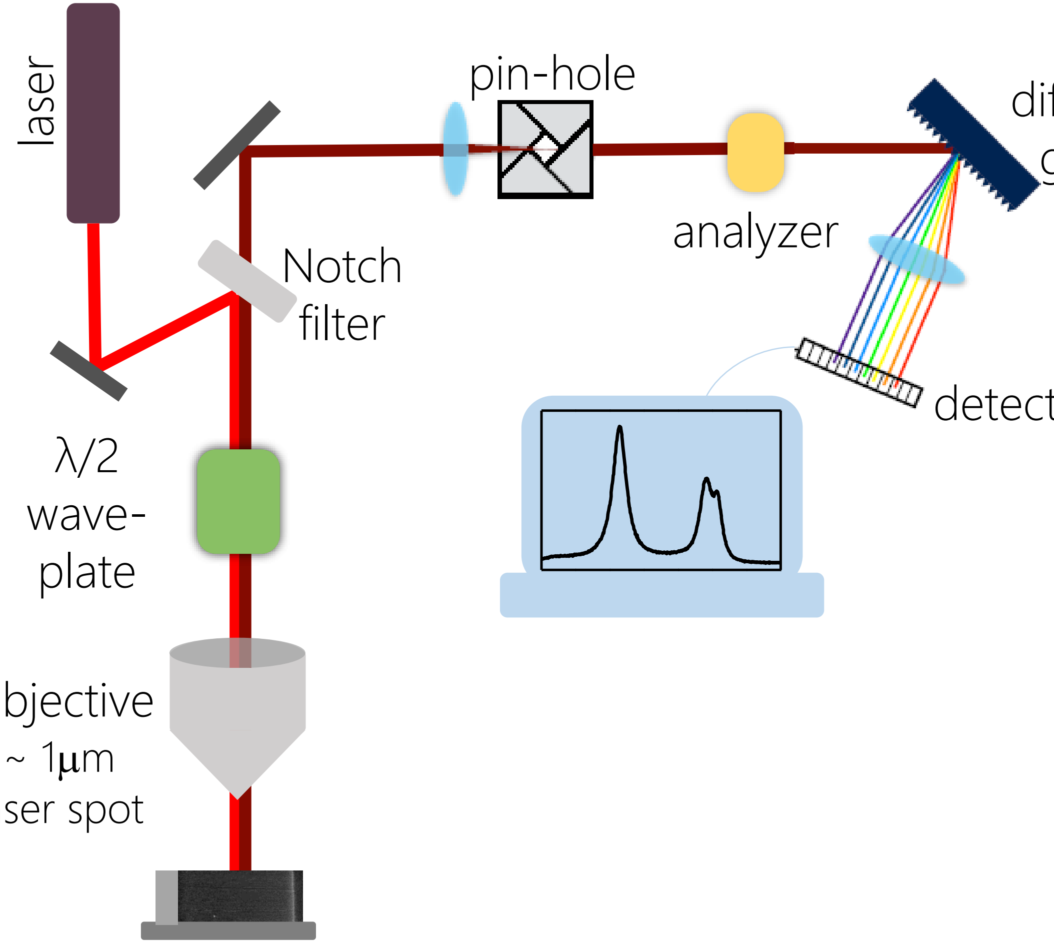

Experimental techniques: Raman spectroscopy

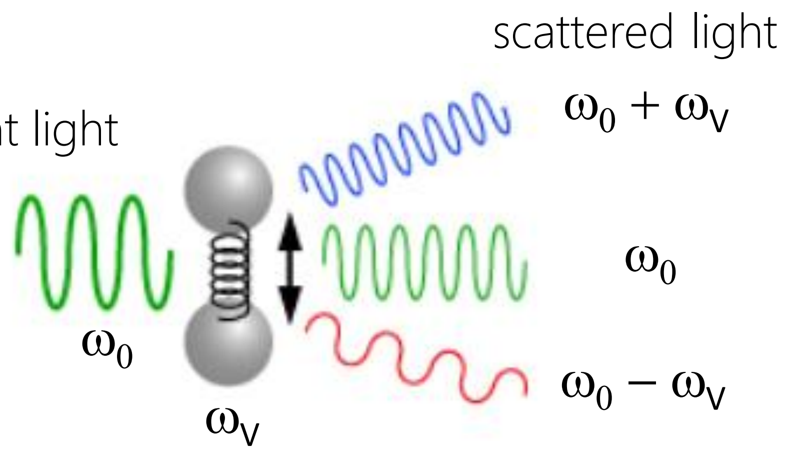

Raman effect: inelastic light scattering

- ✓ vibrational modes ⟷ chemical bonds
- ✓ structural configuration
- ✓ information on the local 'environment'
- ✓ not only surface!
- ✓ possibility of penetration below the surface
- ✓ polarization analysis

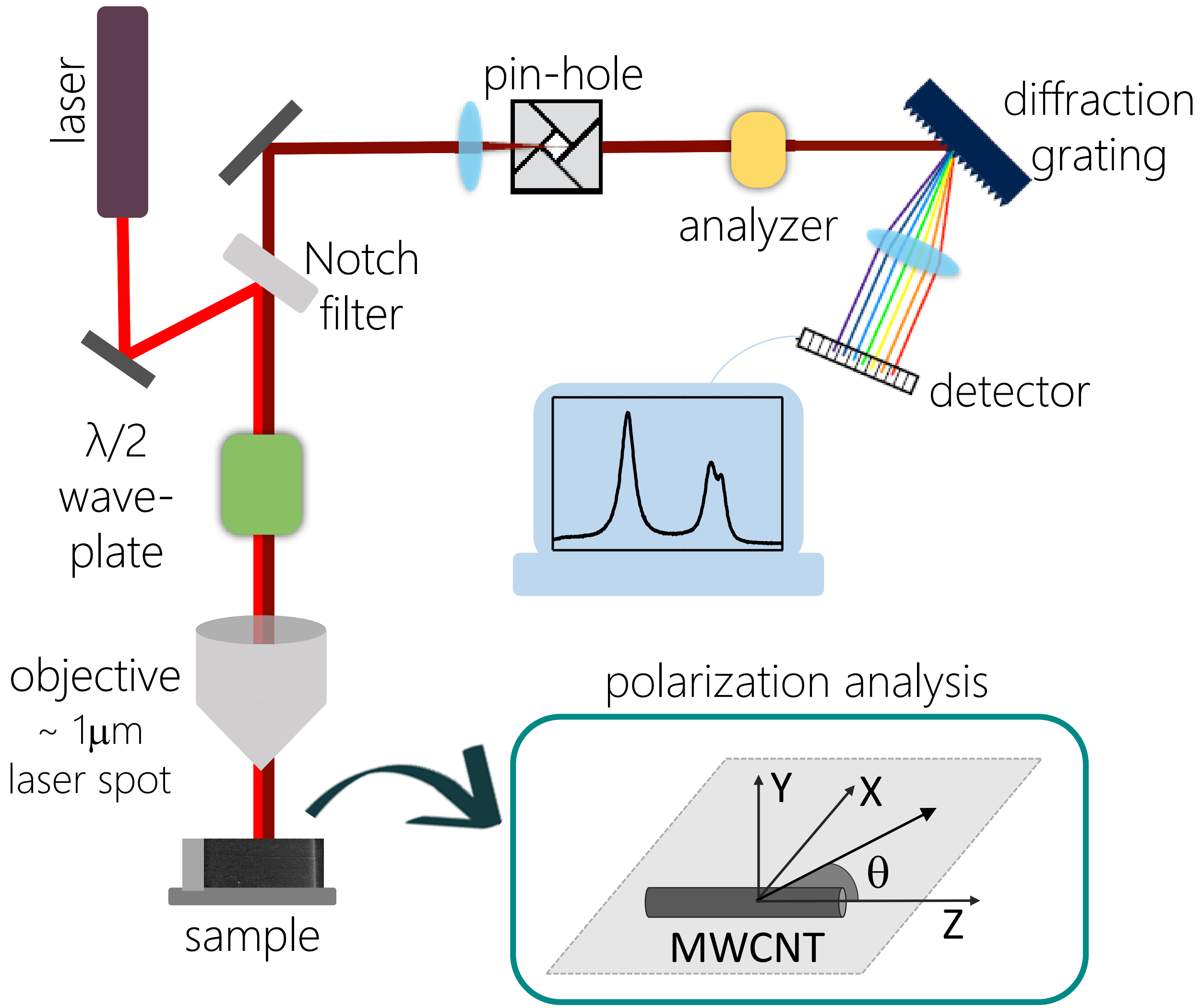

MWCNT growth and characterization

X-ray photoemission spectroscopy @LOTUS group, Sapienza University

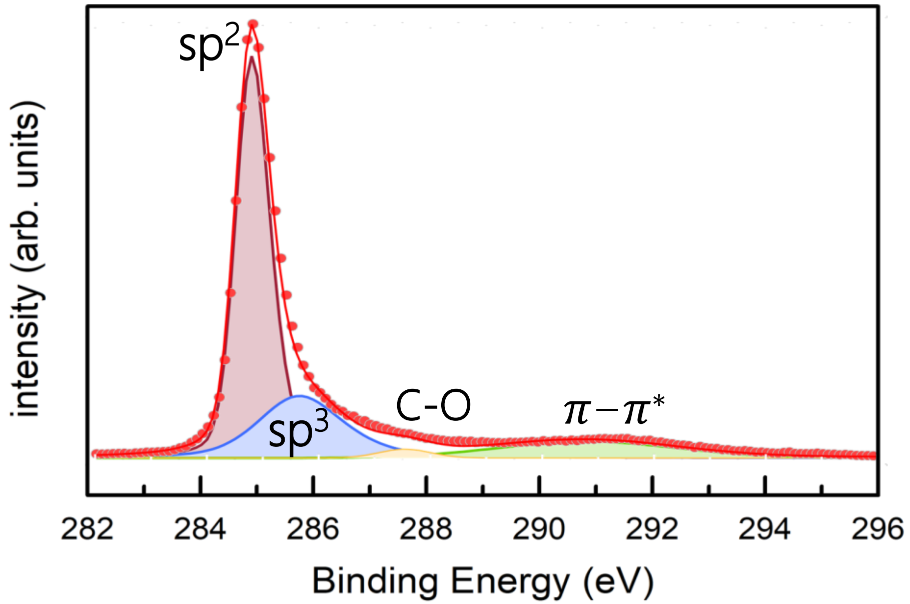

MWCNT growth and characterization

X-ray photoemission spectroscopy @LOTUS group, Sapienza University

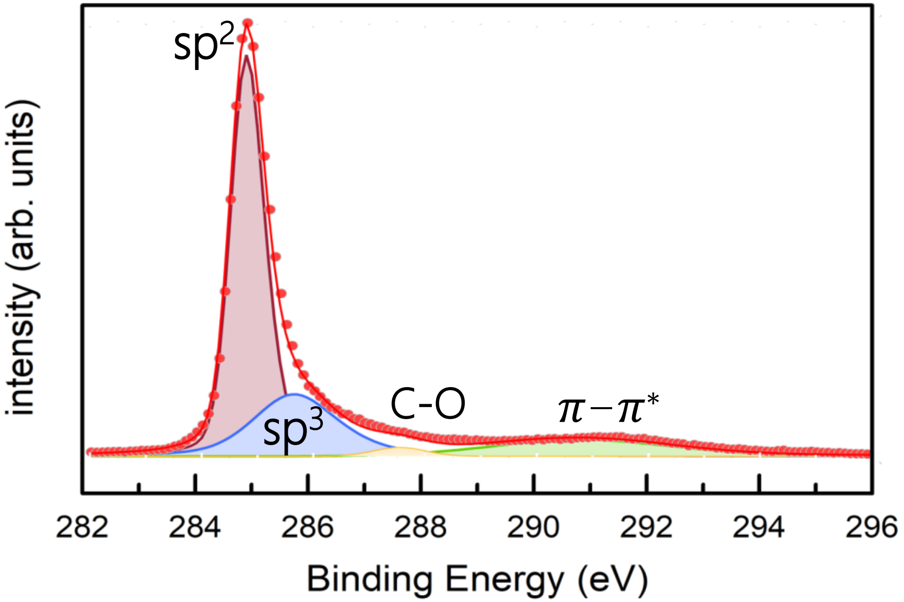

from C 1s core level:

- sp^2 – carbon in perfect hexagonal lattice

planar configuration

MWCNT growth and characterization

X-ray photoemission spectroscopy @LOTUS group, Sapienza University

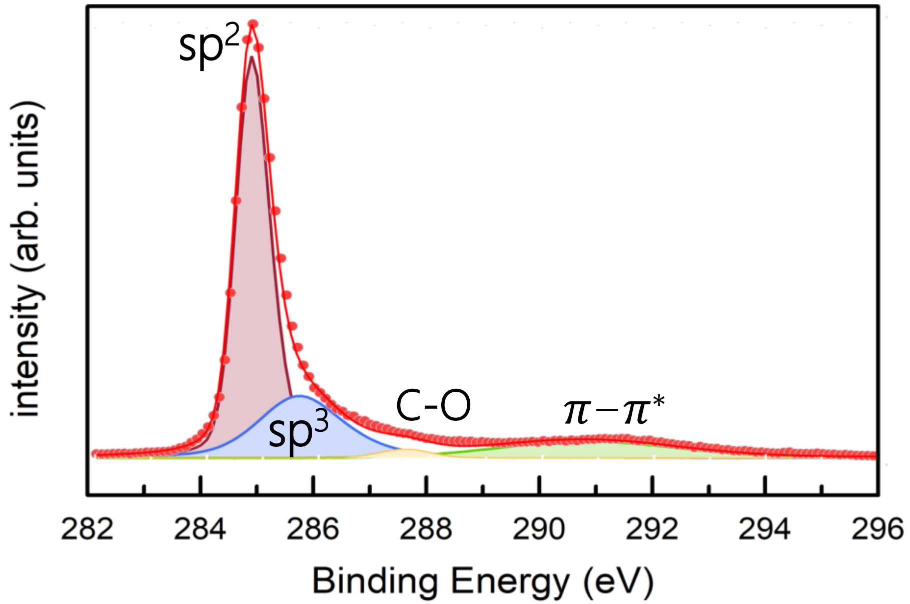

from C 1s core level:

- sp^2 – carbon in perfect hexagonal lattice
- sp^3 like – bond distortion & defect

3D configuration

MWCNT growth and characterization

X-ray photoemission spectroscopy @LOTUS group, Sapienza University

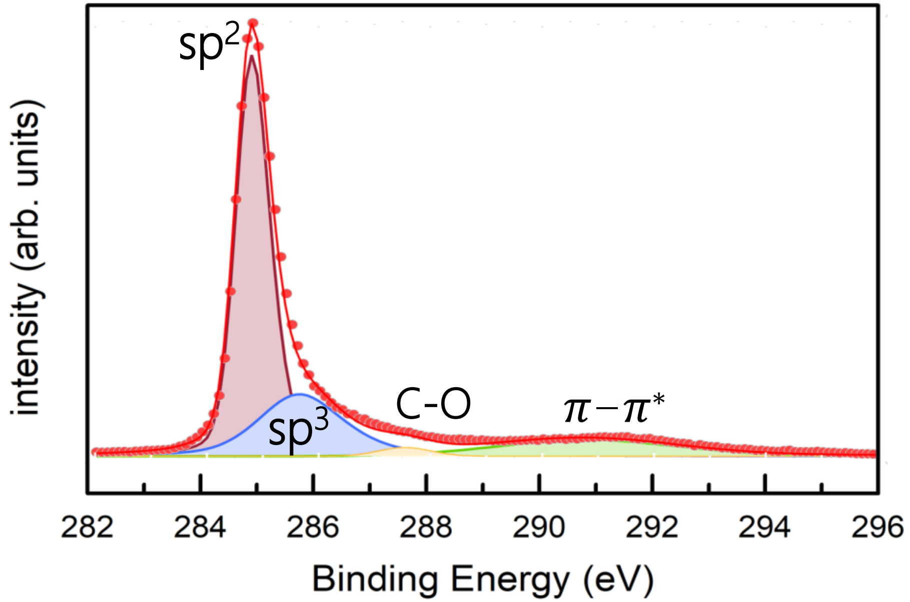

from C 1s core level:

- sp^2 – carbon in perfect hexagonal lattice
- sp^3 like – bond distortion & defect
- $\pi-\pi^*$ transition
- C-O – residual contaminants (less than 2%!)

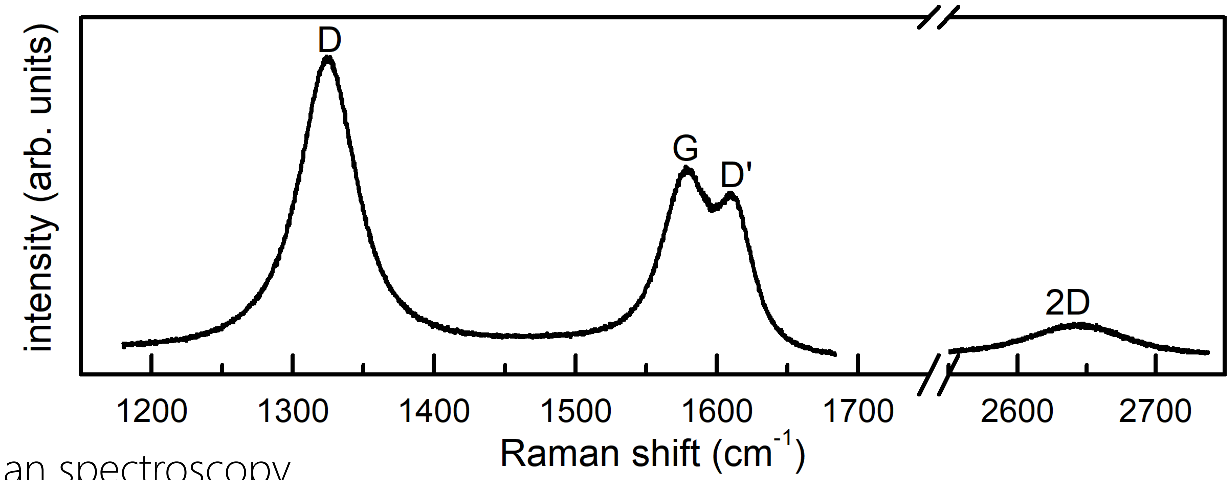

Raman spectroscopy @HPS group, Sapienza University

MWCNT growth and characterization

X-ray photoemission spectroscopy @LOTUS group, Sapienza University

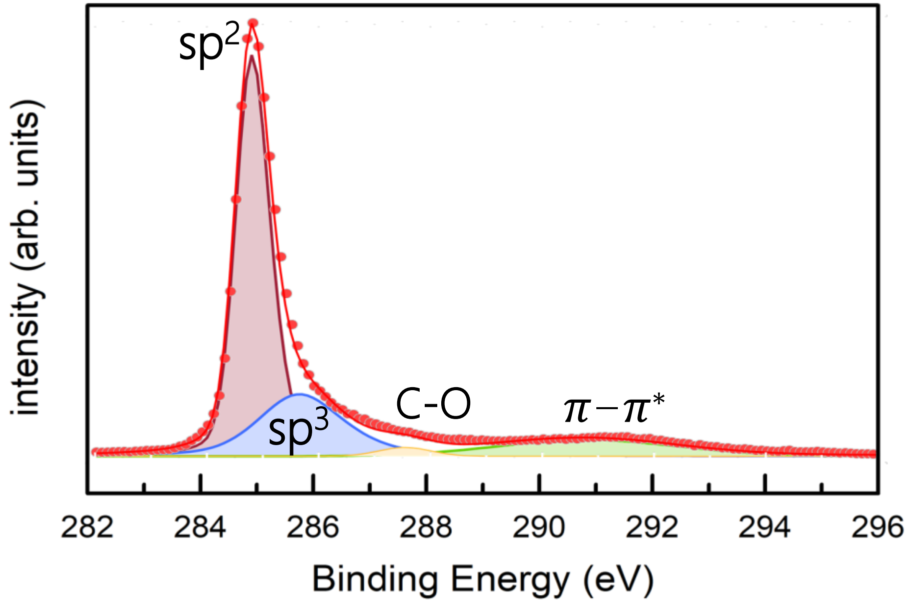

from C 1s core level:

- sp^2 – carbon in perfect hexagonal lattice
- sp^3 like – bond distortion & defect
- $\pi-\pi^*$ transition
- C-O – residual contaminants (less than 2%!)

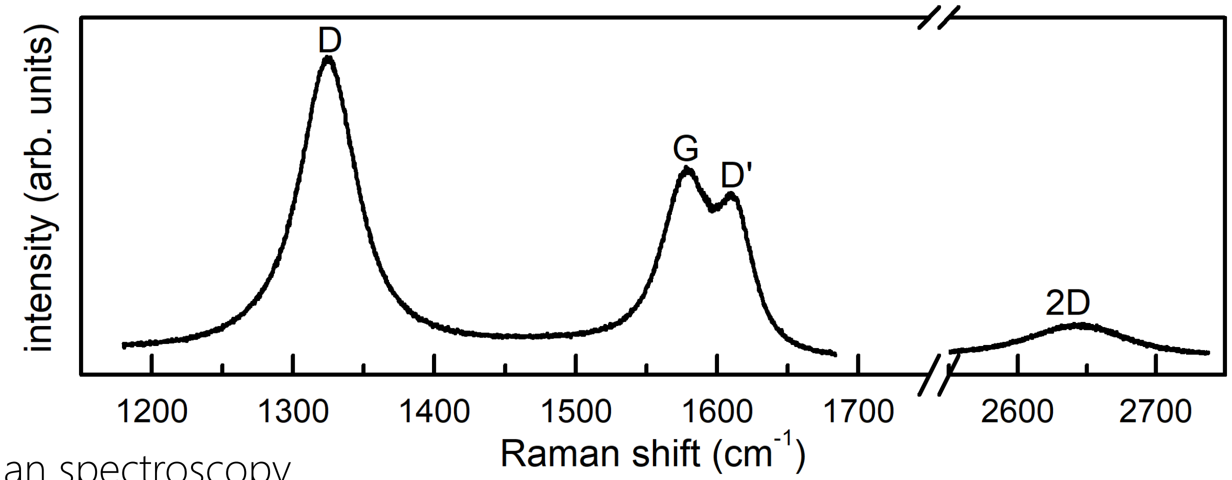

Raman spectroscopy @HPS group, Sapienza University

from Raman spectrum:

- D – lattice defect (curvature effect)
- G – sp^2 C-C stretching
- D′ – bond distortion (curvature effect)
- 2D – hexagonal ring breathing (lattice)

MWCNT growth and characterization

X-ray photoemission spectroscopy @LOTUS group, Sapienza University

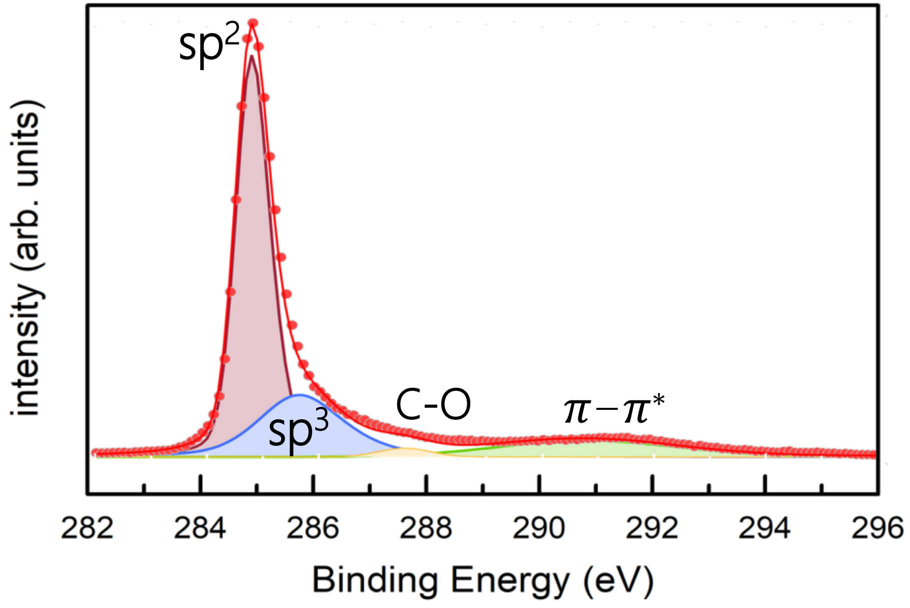

from C 1s core level:

- sp^2 – carbon in perfect hexagonal lattice
- sp^3 like – bond distortion & defect
- $\pi-\pi^*$ transition
- C-O – residual contaminants (less than 2%!)

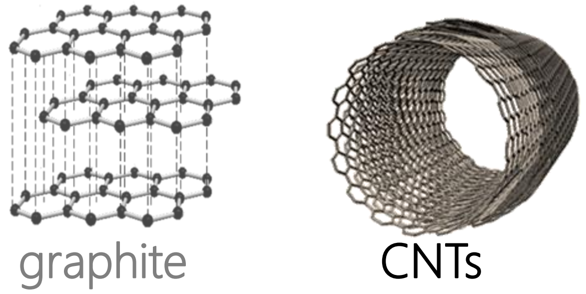

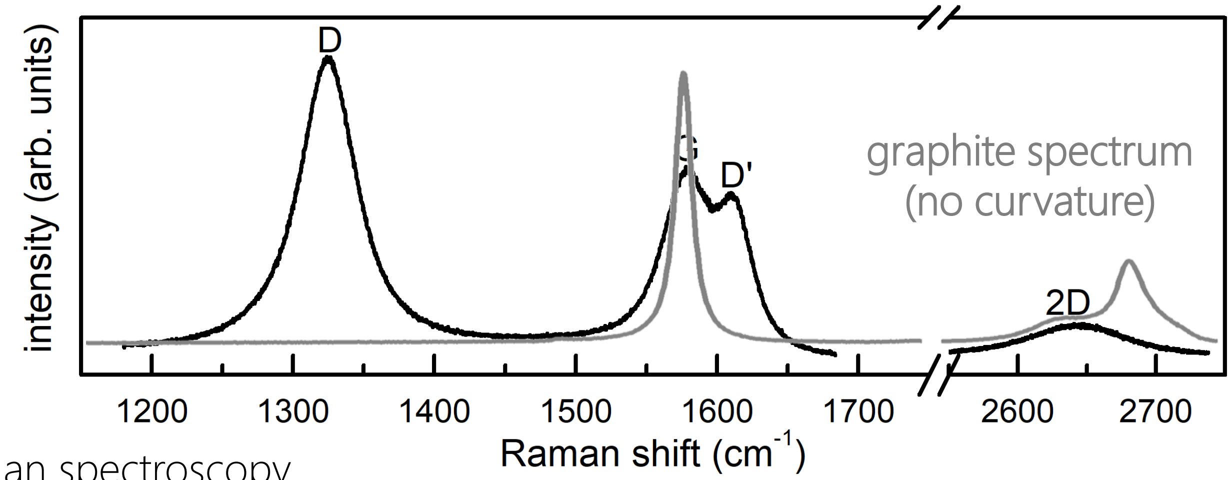

Raman spectroscopy @HPS group, Sapienza University

from Raman spectrum:

- D – lattice defect (**curvature effect**)
- G – sp^2 C-C stretching
- D′ – bond distortion (**curvature effect**)
- 2D – hexagonal ring breathing (lattice)

Ion bombardment: Raman spectroscopy

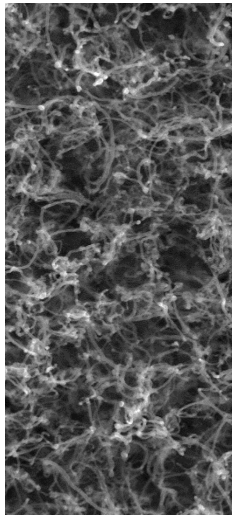

before
bombardment

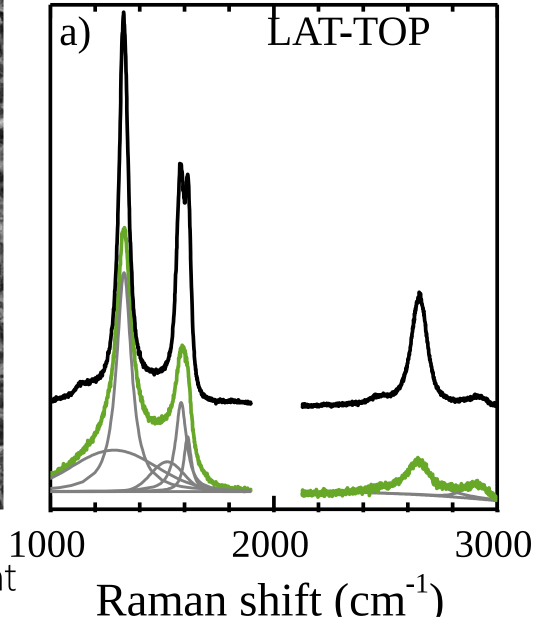

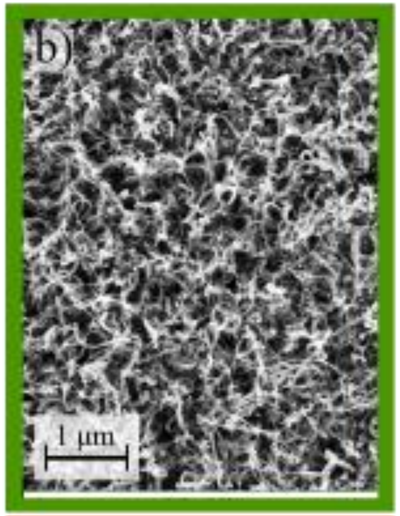

after
bombardment

bombardment direction

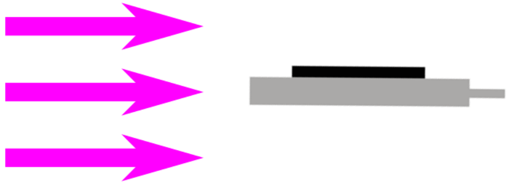

measurement direction

G. D'Acunto, F. Ripanti, et al., Carbon 139, 768, 2018

Ion bombardment: Raman spectroscopy

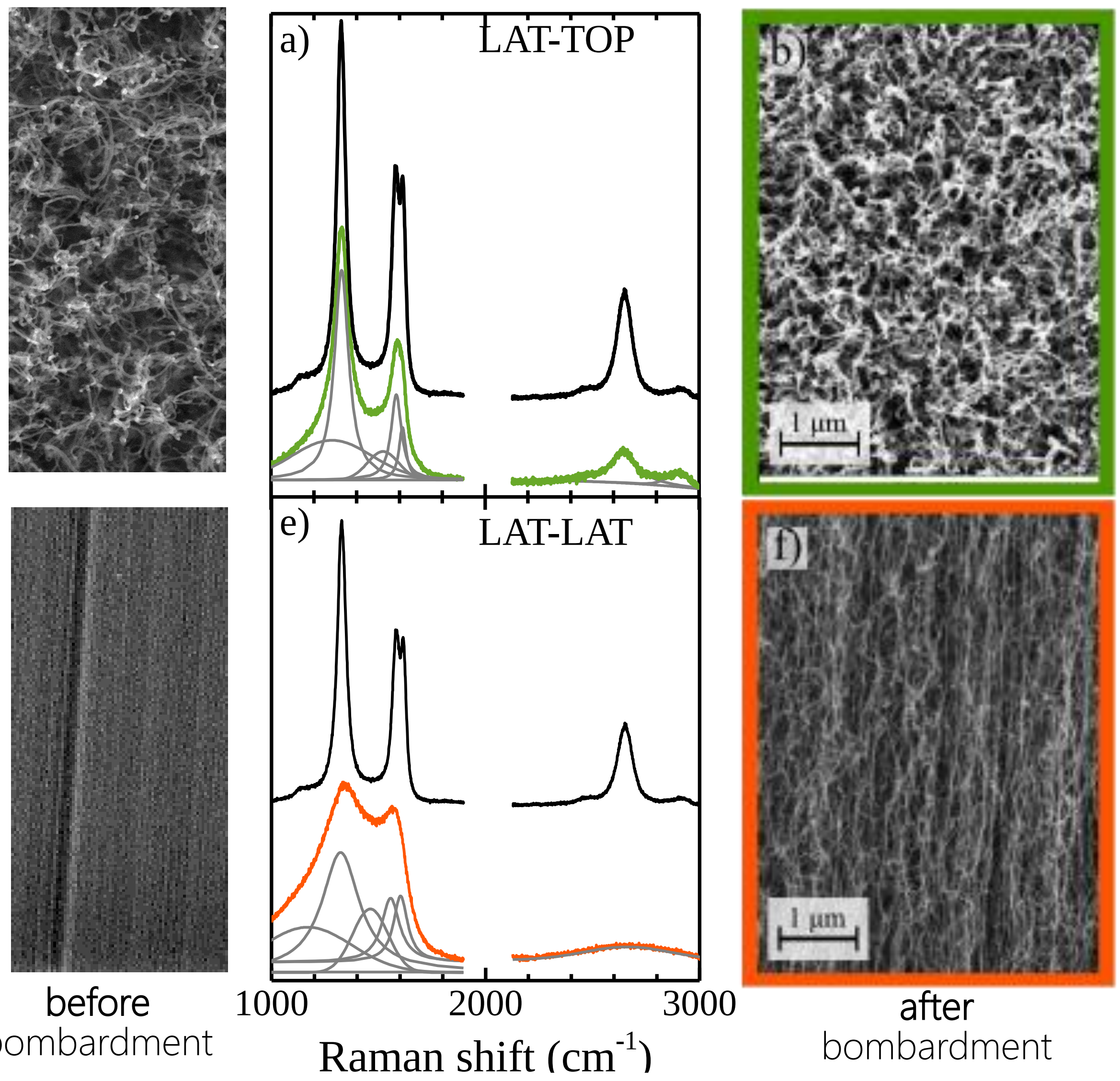

before bombardment

after bombardment

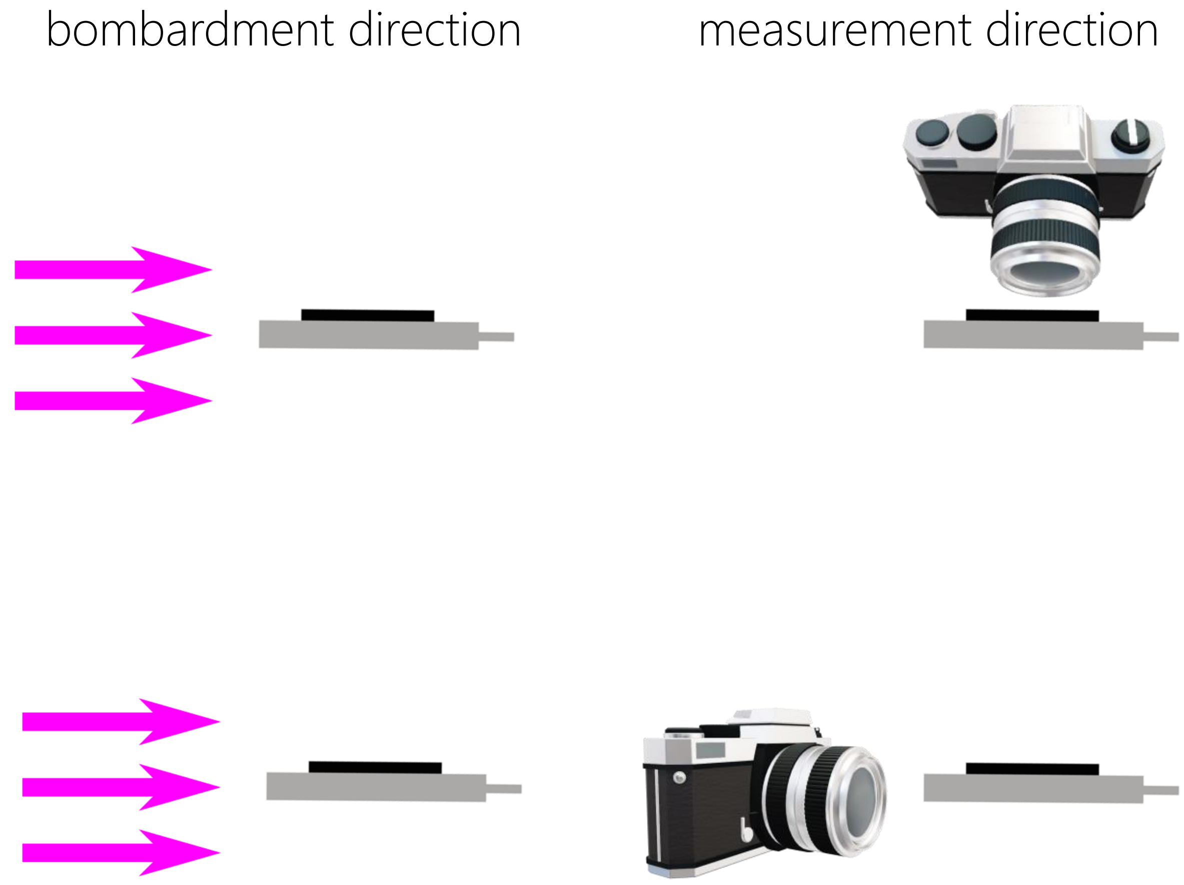

G. D'Acunto, F. Ripanti, et al., Carbon 139, 768, 2018

Ion bombardment: Raman spectroscopy

bombardment direction

measurement direction

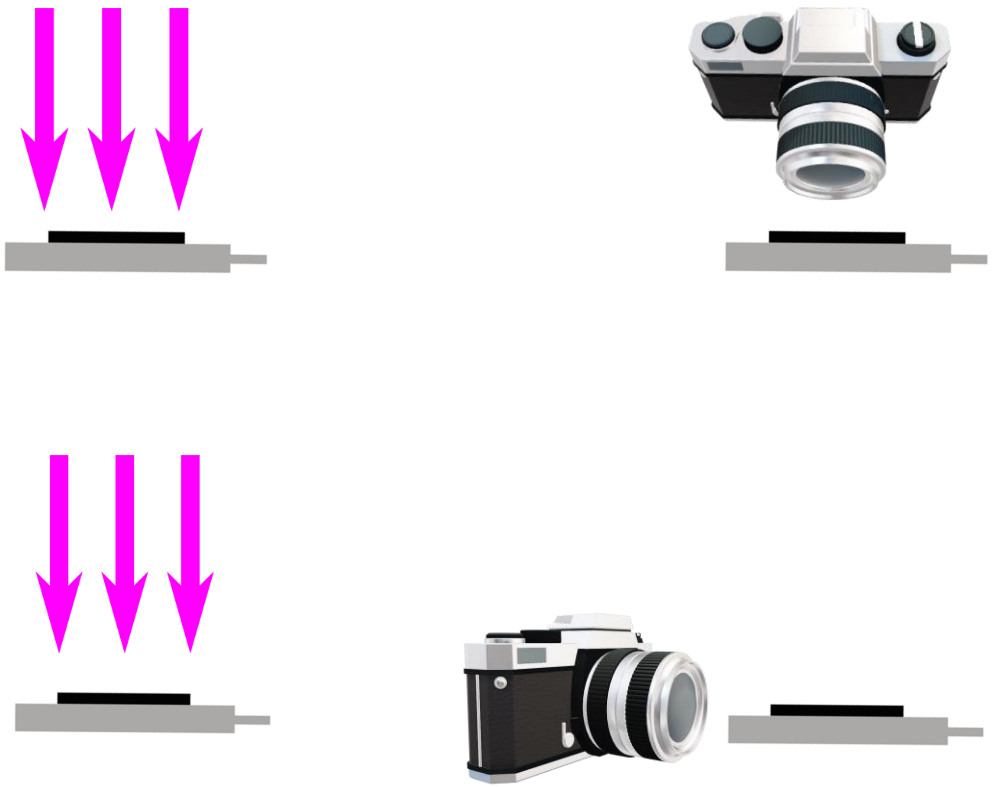

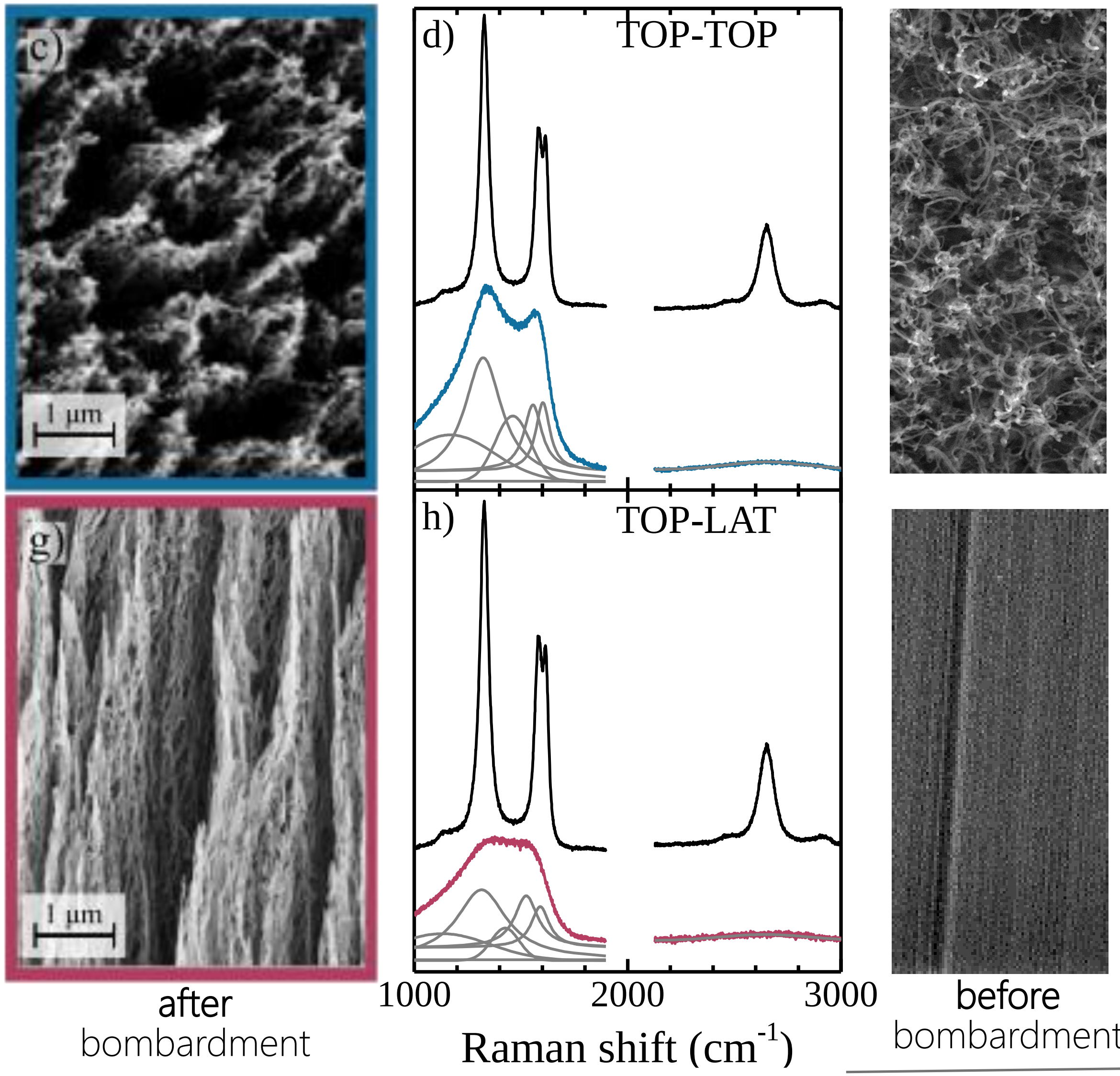

after bombardment

before bombardment

Francesca Ripanti

G. D'Acunto, F. Ripanti, et al., Carbon 139, 768, 2018

Ion bombardment: Raman spectroscopy

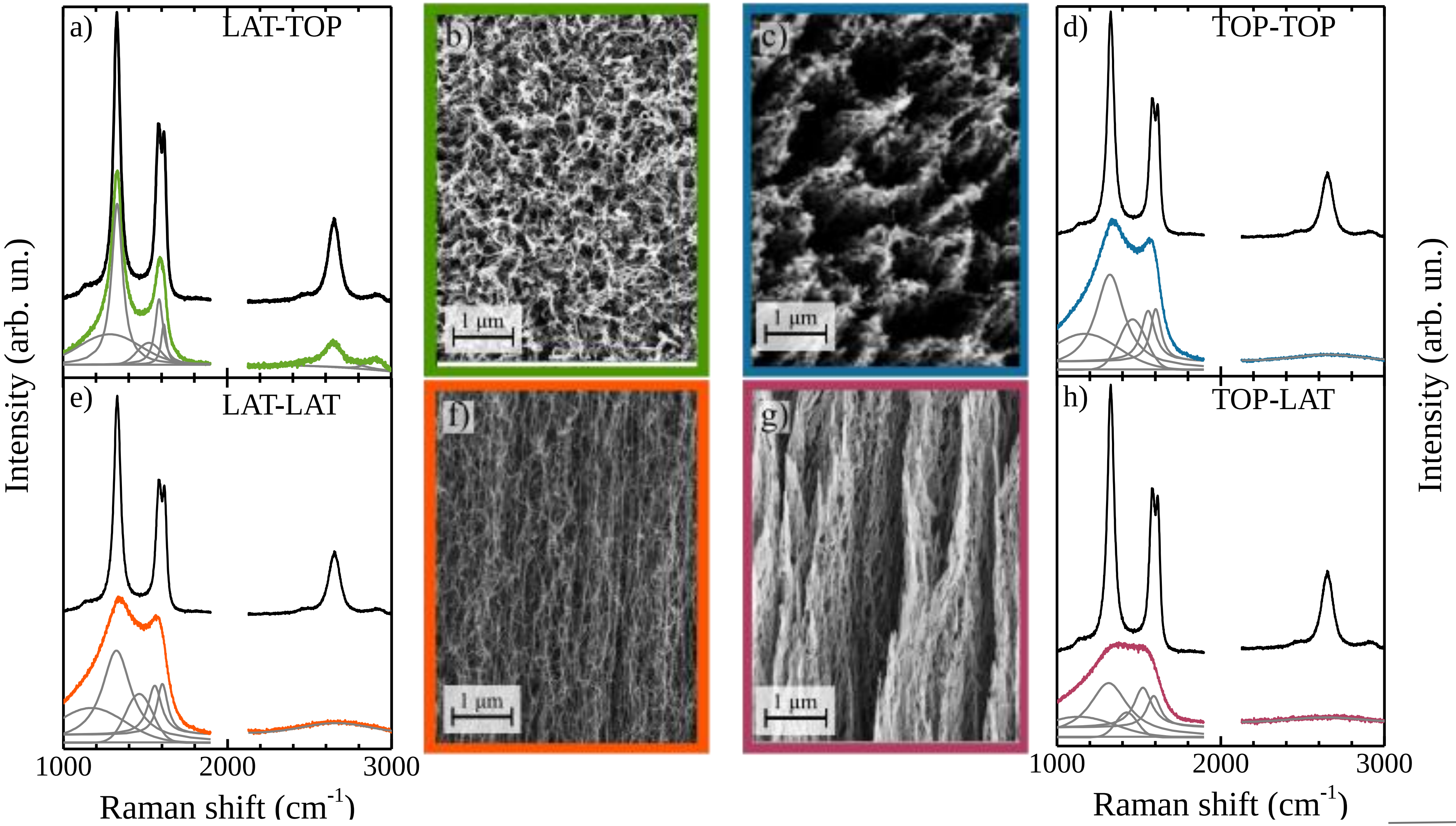

G. D'Acunto, F. Ripanti, et al., Carbon 139, 768, 2018

Ion bombardment: XPS spectroscopy

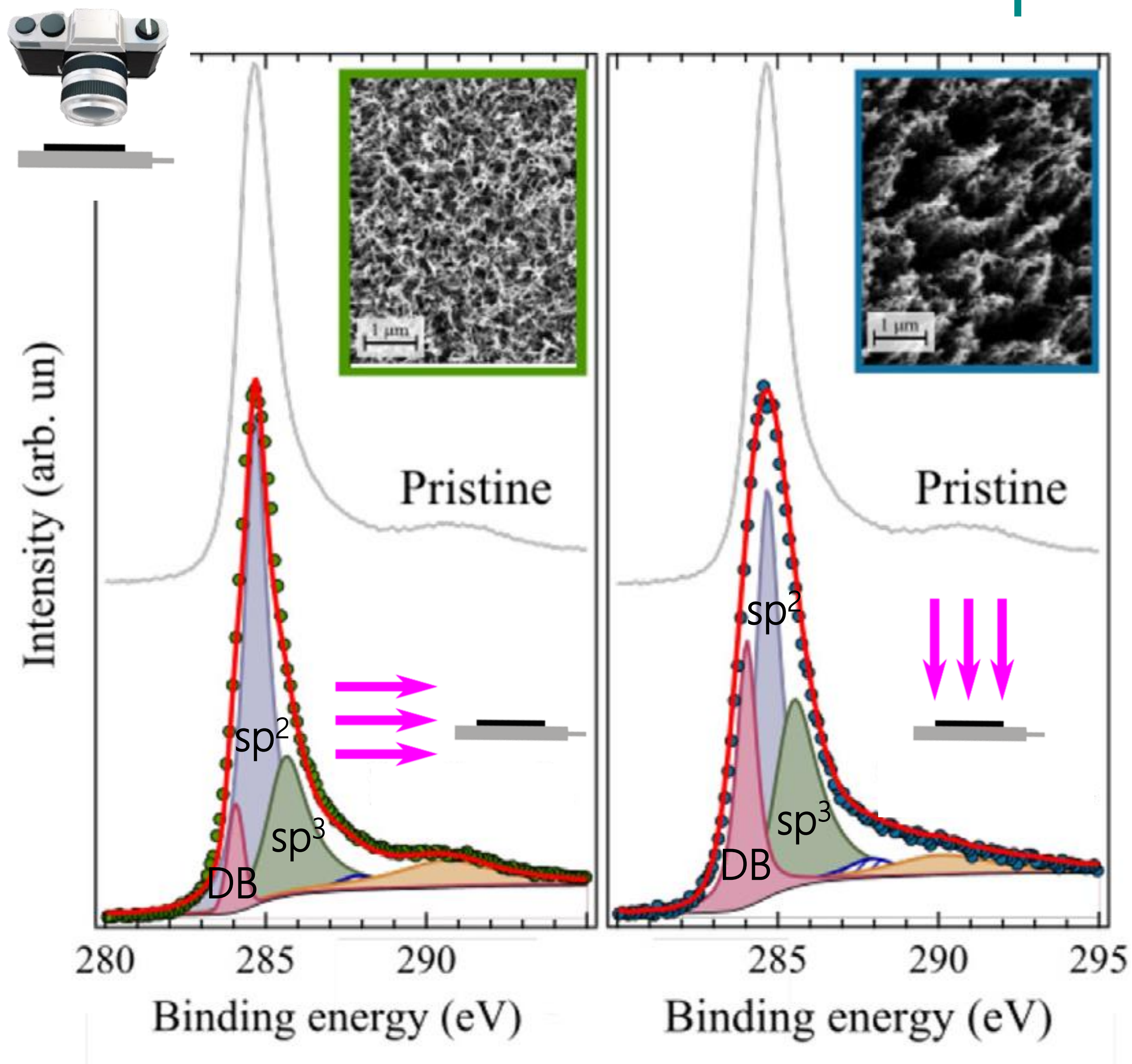

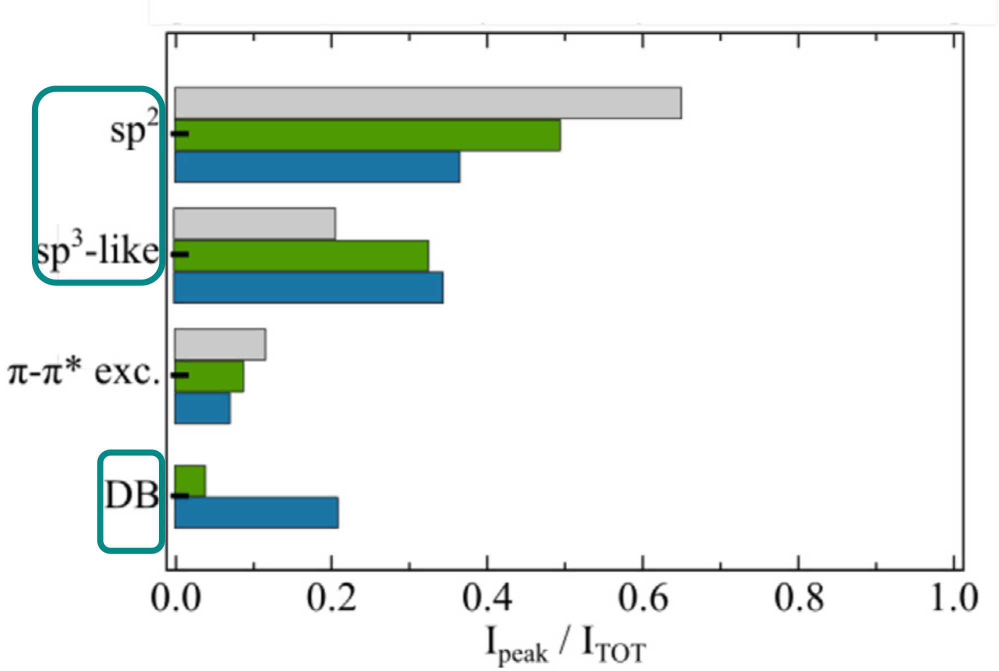

from XPS C 1s spectrum of bombarded tubes:

- ✓ different peaks associated to different C configurations (defects)
- ✓ percentage of each peak
- ✓ evaluate the nature of the defects present in the two different cases

G. D'Acunto, F. Ripanti, et al., Carbon 139, 768, 2018

Ion bombardment: depth analysis

Raman spectroscopy allows measurements below the surface at different depths into the MWCNT forest

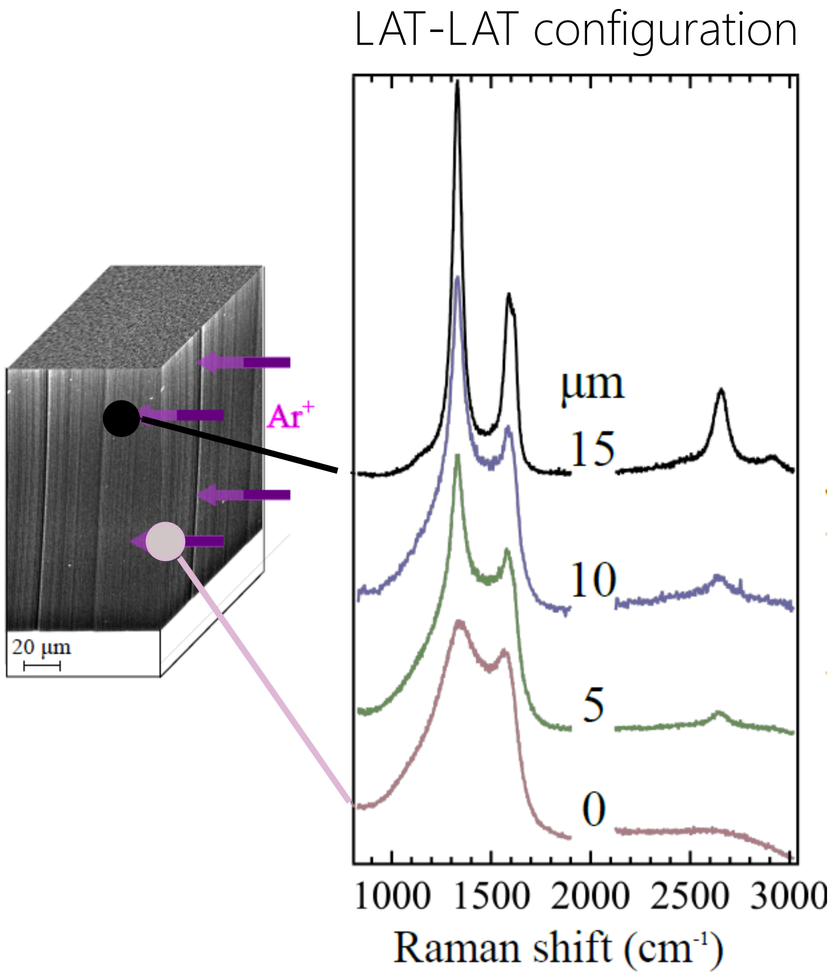

- ✓ the amorphization is clearly evident on the surface
- ✓ the damage is arrested down to 10 µm of laser probe focalization

G. D'Acunto, F. Ripanti, et al., *Carbon* 139, 768, 2018

Ion bombardment: depth analysis

Raman spectroscopy allows measurements below the surface at different depths into the MWCNT forest

LAT-LAT configuration

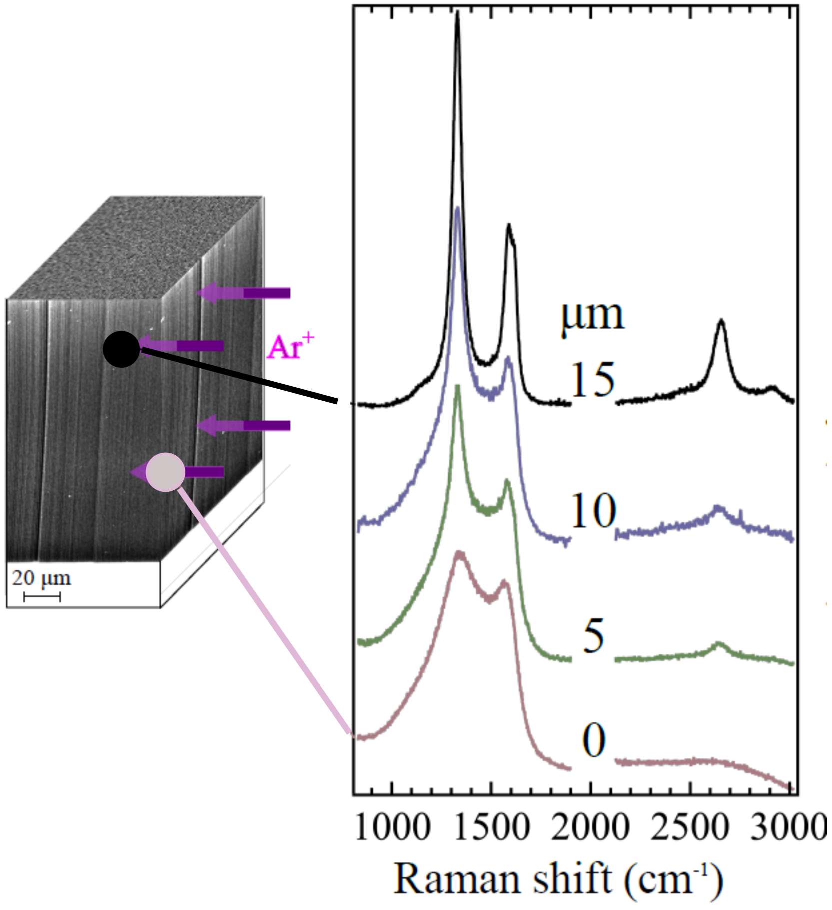

- ✓ the amorphization is clearly evident on the surface
- ✓ the damage is arrested down to 10 μm of laser probe focalization
- ✓ same shape on the lateral surface along the whole CNT axis

preferential ion channeling parallel to the tube axis

TOP-LAT configuration

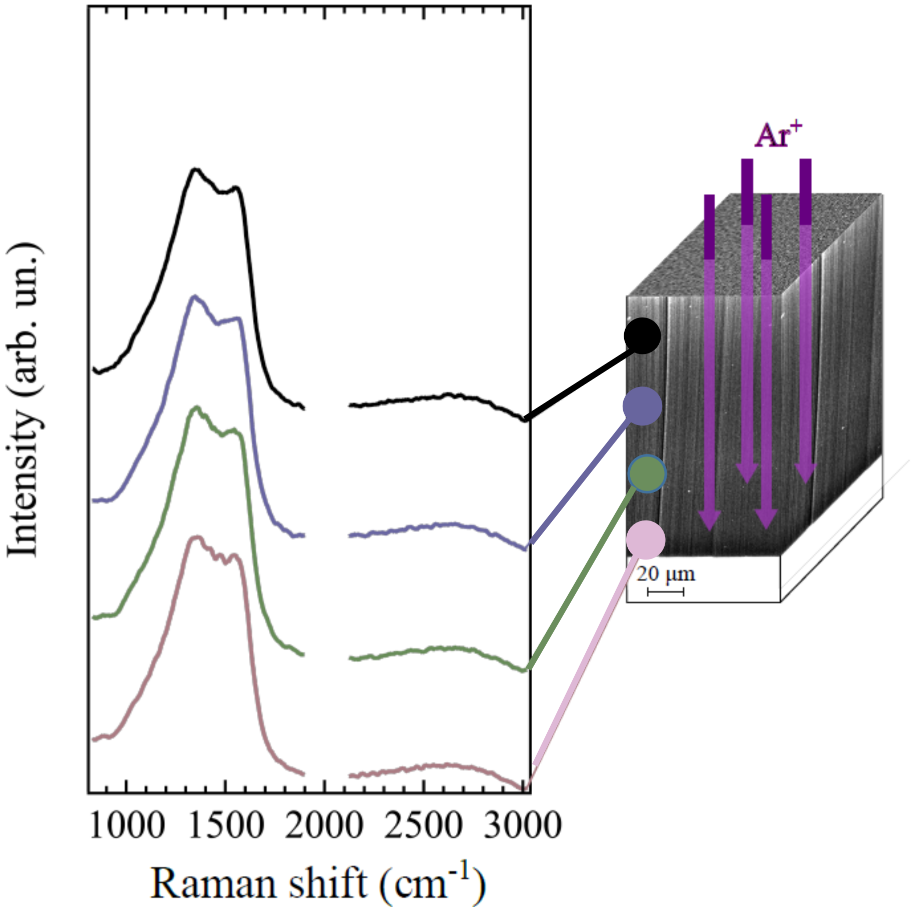

G. D'Acunto, F. Ripanti, et al., Carbon 139, 768, 2018

Ion bombardment at different angles

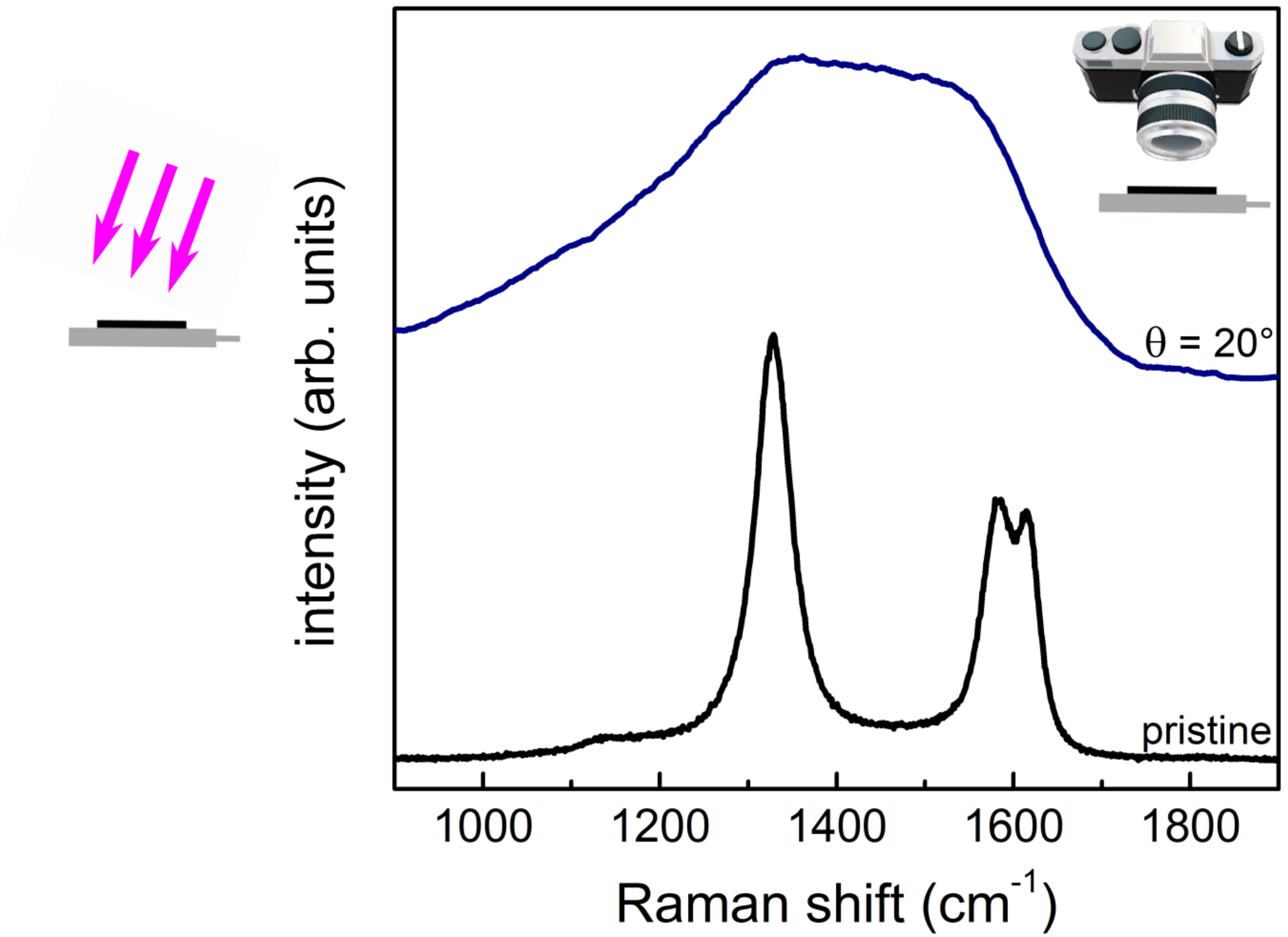

Ion bombardment at different angles

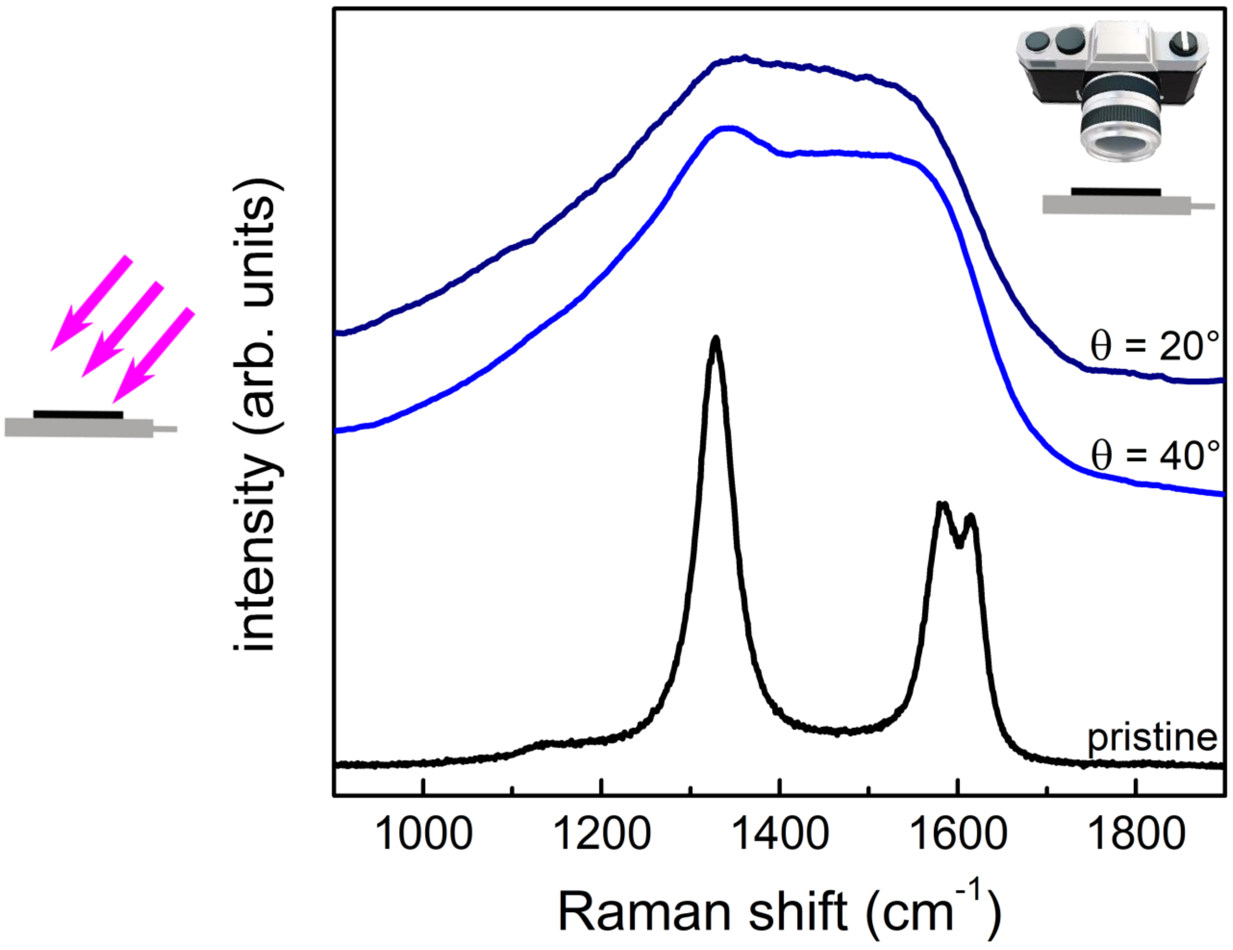

Ion bombardment at different angles

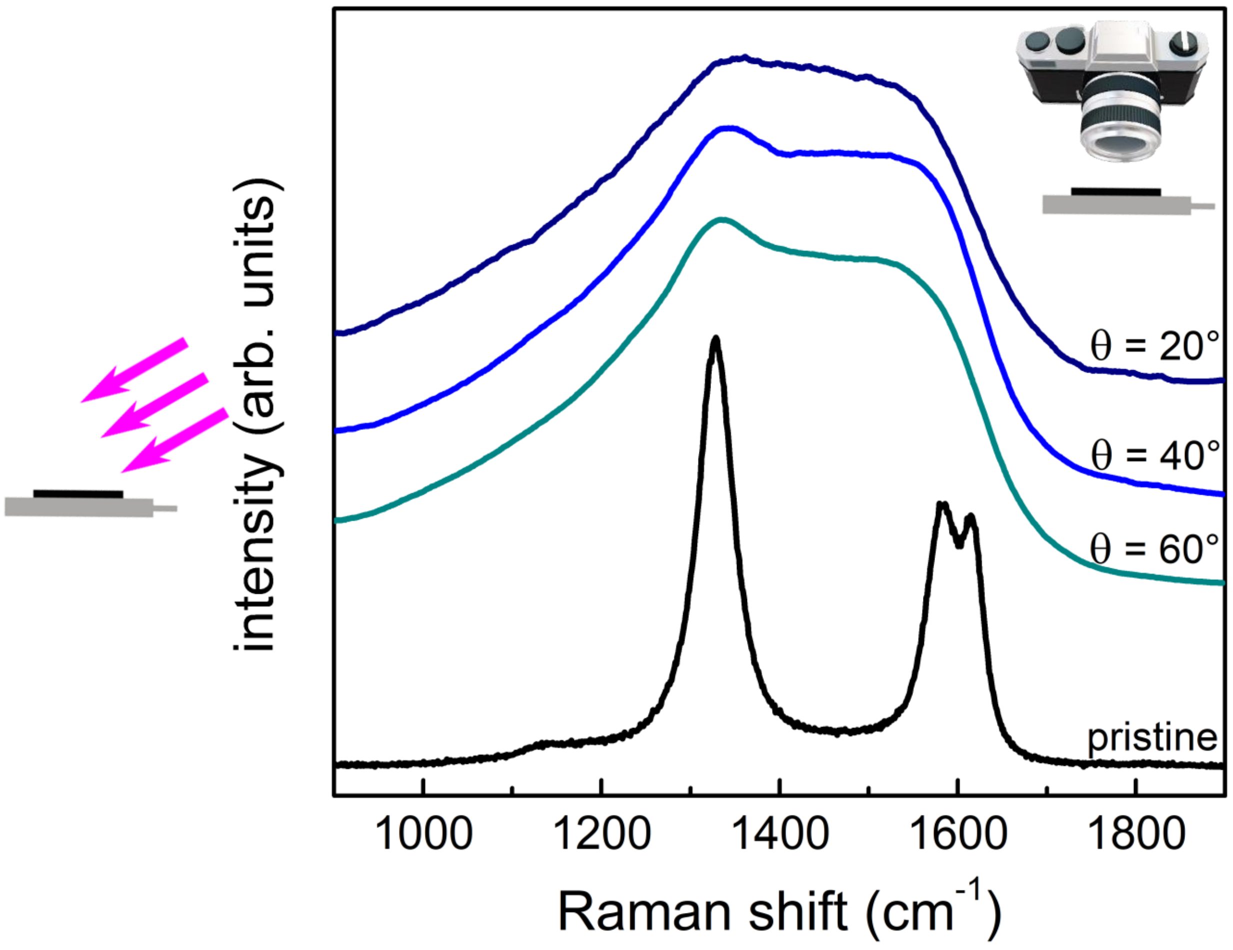

Ion bombardment at different angles

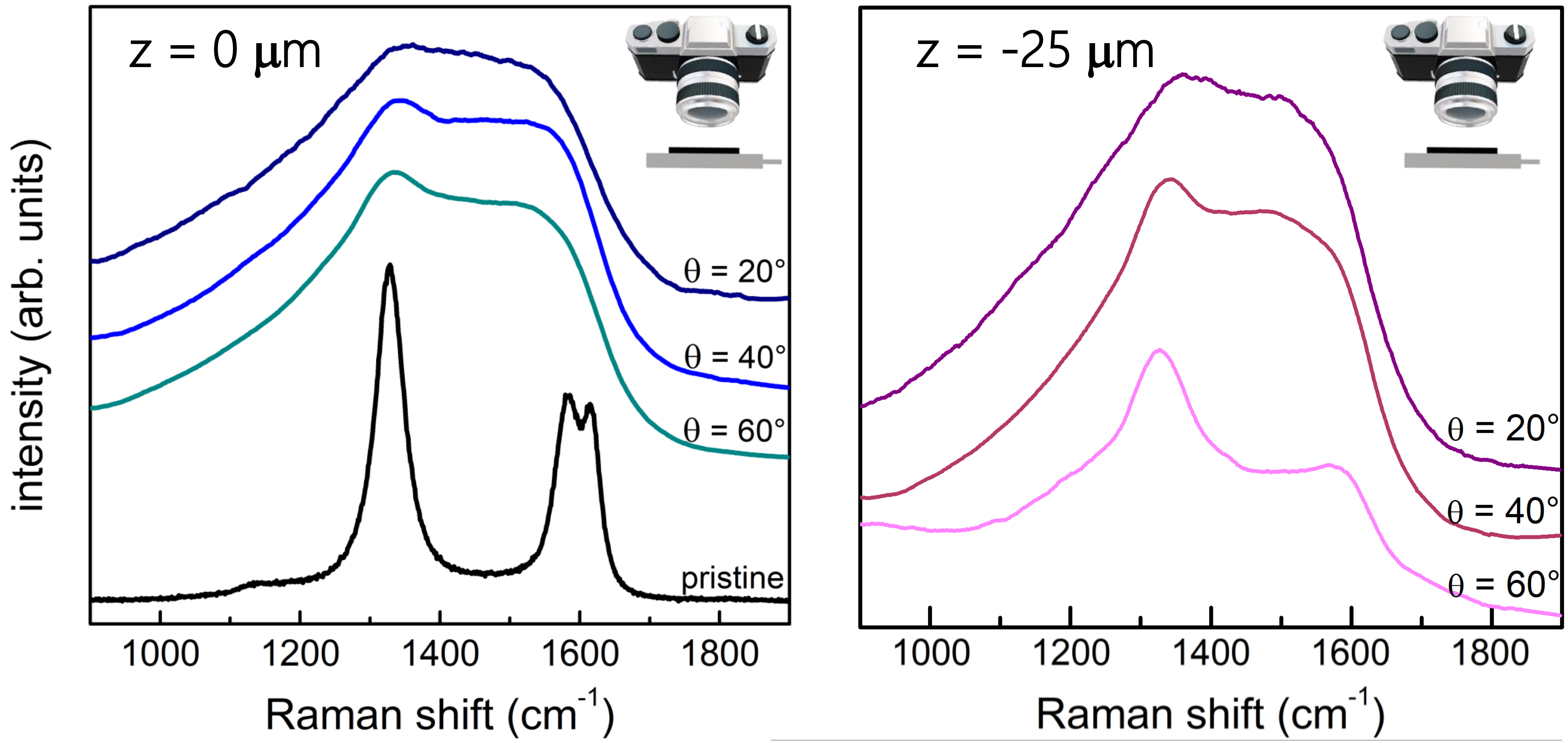

critical angle?
ongoing project: simulations by E. Bernabei, G. Cavoto

- ✓ damage dependent on the bombardment angle
- ✓ above 40° the amorphization level decreases varying the depth

Ion bombardment: remarks

aim: study of the **directional** bombardment of CNTs

- CNT array is a highly anisotropic system
- Ar^{+} ion bombardment at different angles
- XPS and Raman spectroscopy to demonstrate the directional effects

✓ preferential ion channeling parallel to the tube axis
✓ possible critical angle above 40°?

Ion bombardment: remarks

aim: study of the **directional** bombardment of CNTs

- CNT array is a highly anisotropic system
- Ar^+ ion bombardment at different angles
- XPS and Raman spectroscopy to demonstrate the directional effects

✓ preferential ion channeling parallel to the tube axis
✓ possible critical angle above 40°?

how do these results depend on the sample quality?
is the nanotube direction well defined?

Polarization analysis: basic idea

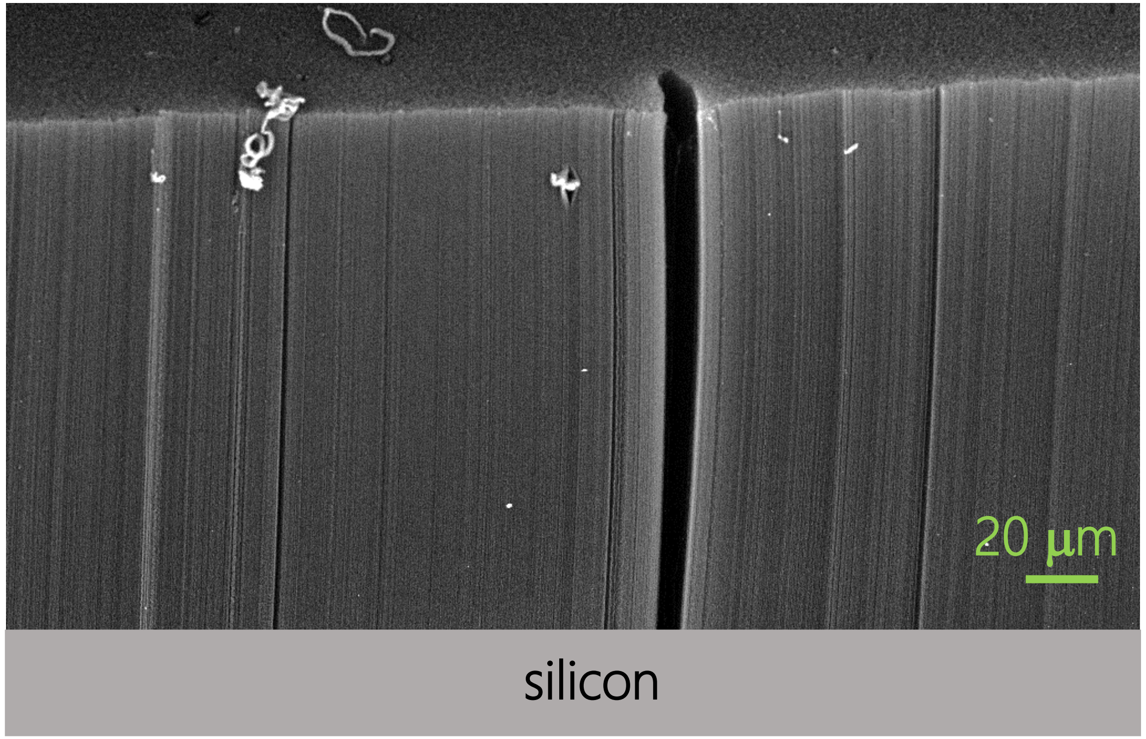

Polarization analysis: basic idea

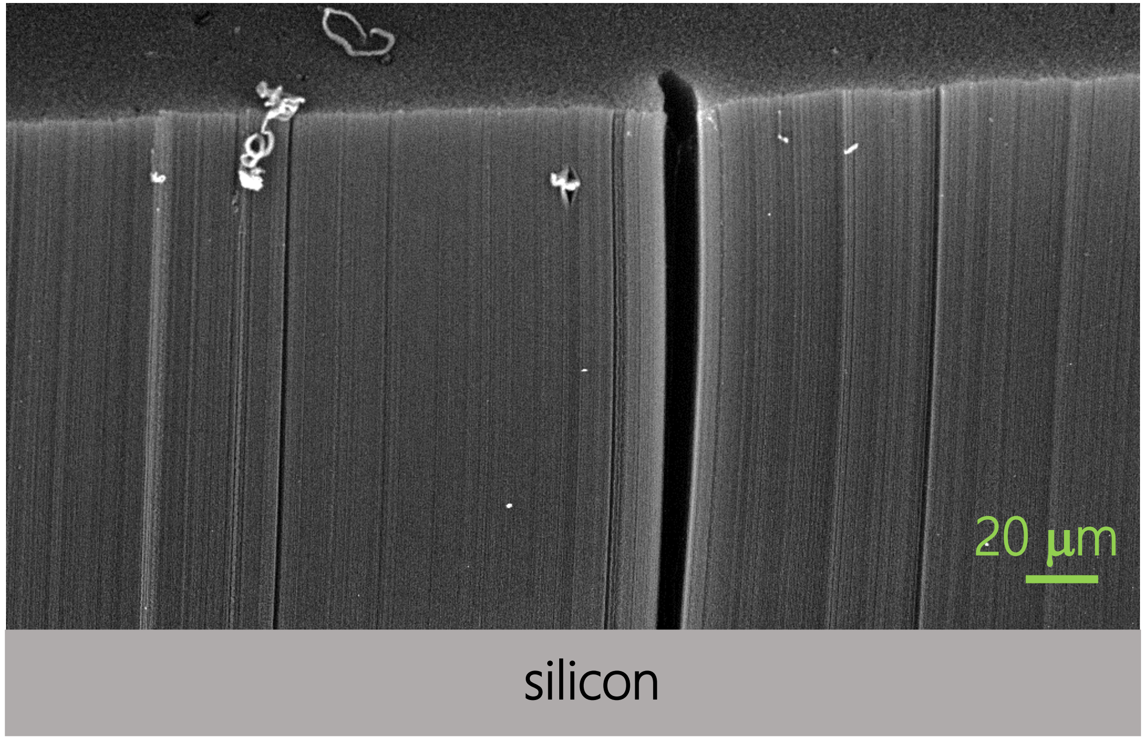

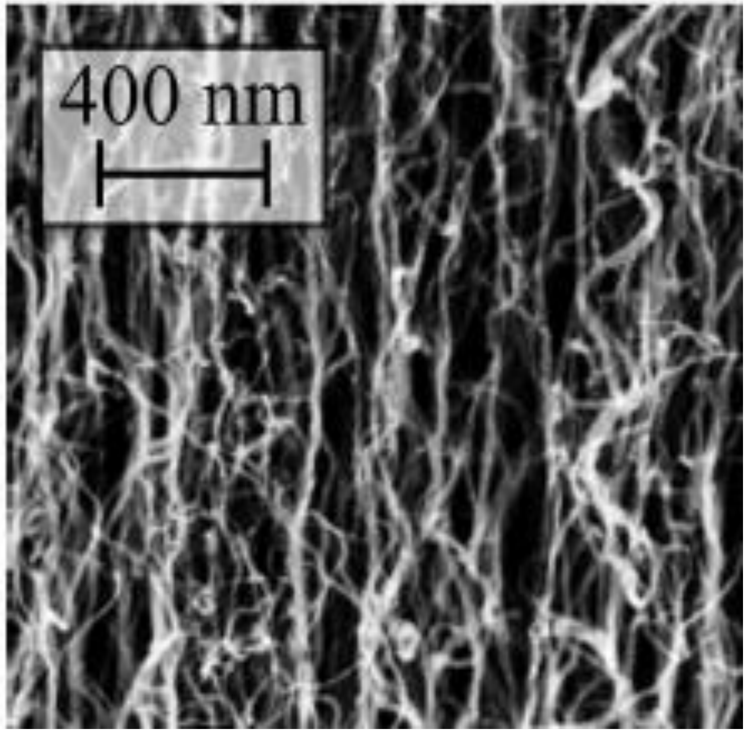

highly aligned vertical MWCNTs on a large scale

on a smaller spatial scale, they appear misaligned with respect to the average tube axis direction

Polarization analysis: basic idea

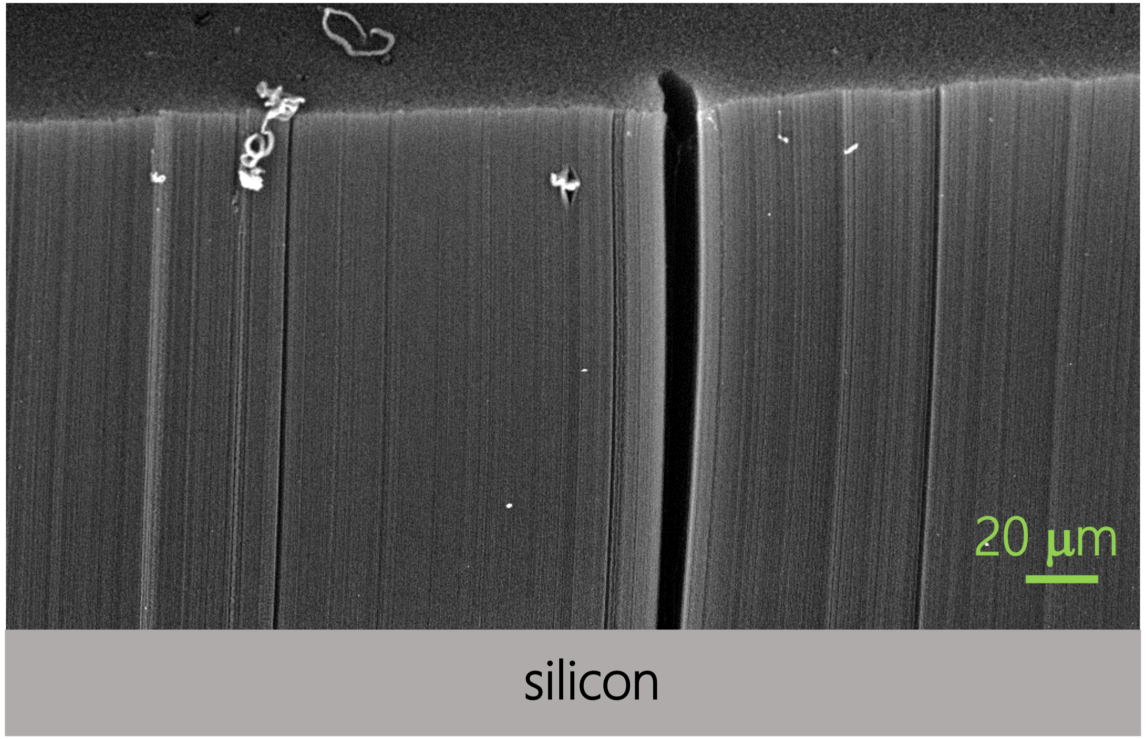

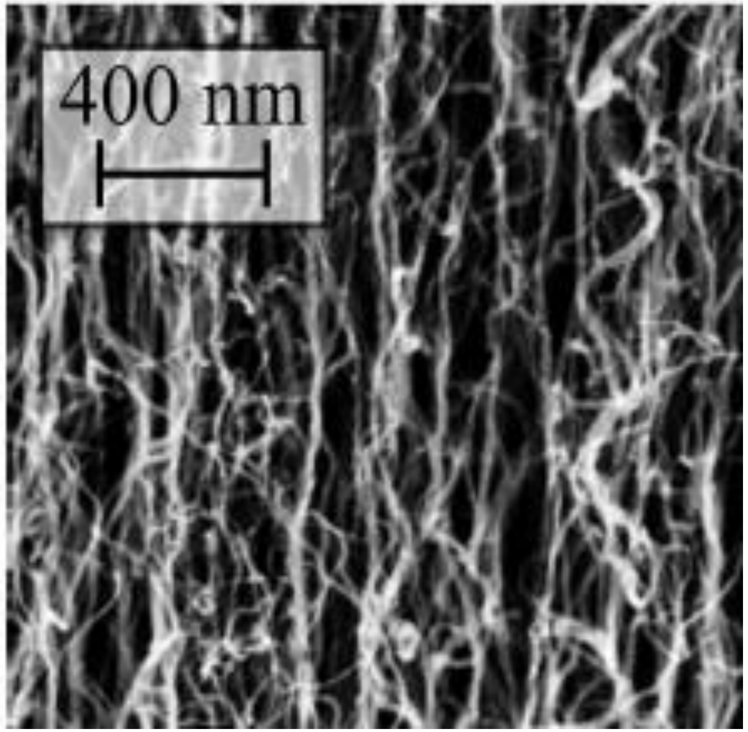

highly aligned vertical MWCNTs on a large scale

on a smaller spatial scale, they appear misaligned with respect to the average tube axis direction

experimental strategy

- determine the dependence on the CNT axis alignment
- Raman polarization analysis
- well defined oscillating direction of the electromagnetic field
- angle between polarization vector and vertical axis

Polarization analysis

from Raman standard theory $I \propto |\varepsilon_i \cdot R \cdot \varepsilon_s|^2$

polarization vector of the incident radiation

polarization vector of the scattered radiation

in our case:

- backscattering configuration $\boldsymbol{k}_i = \boldsymbol{k}_s$
- varying the polarization with an half-waveplate $\boldsymbol{\varepsilon}_i = \boldsymbol{\varepsilon}_s$

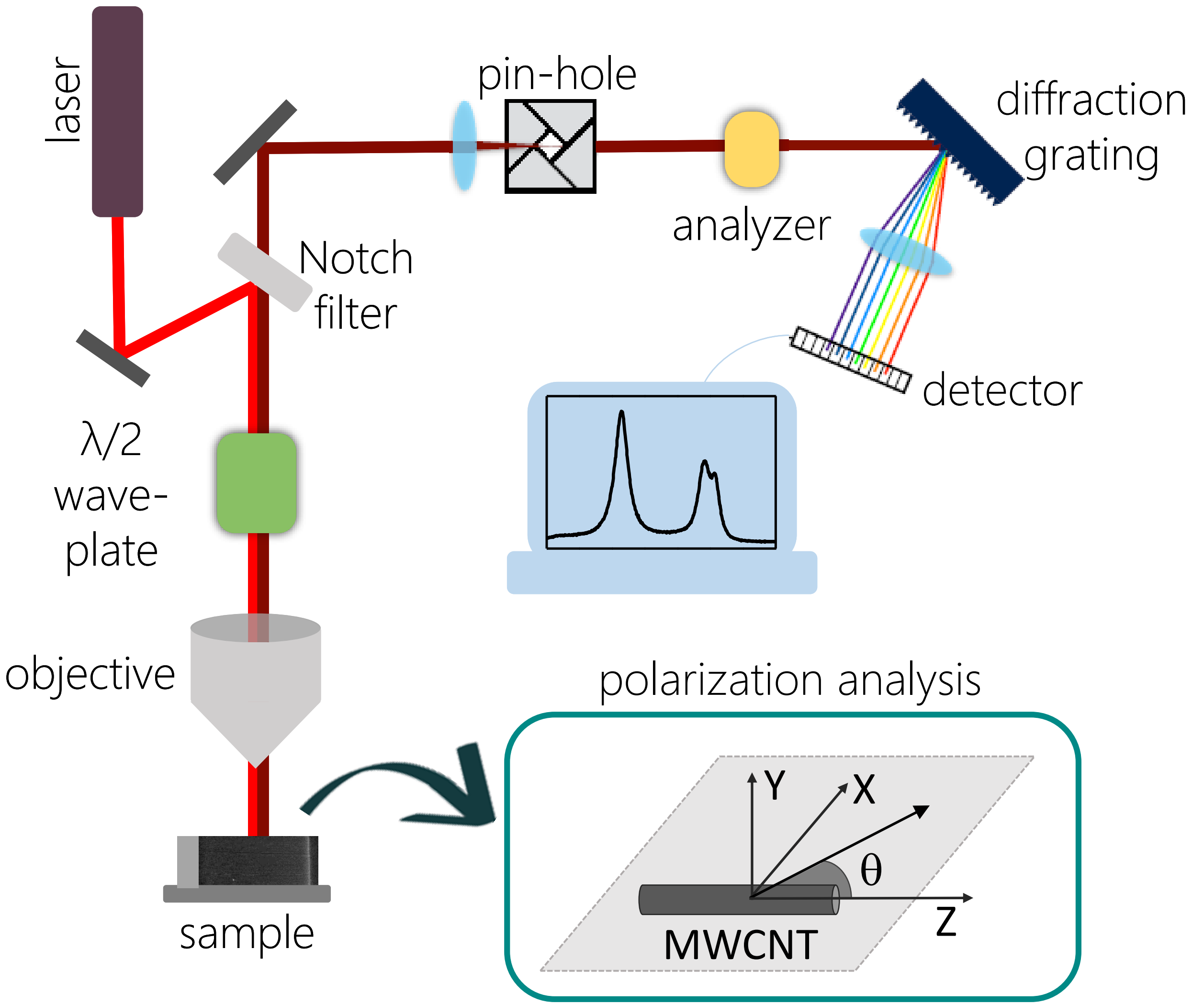

Polarization analysis

from Raman standard theory $I \propto |\varepsilon_i \cdot R \cdot \varepsilon_s|^2$

polarization vector of the incident radiation

polarization vector of the scattered radiation

in our case:

- backscattering configuration $\boldsymbol{k}_i = \boldsymbol{k}_s$
- varying the polarization with an half-waveplate $\boldsymbol{\varepsilon}_i = \boldsymbol{\varepsilon}_s$

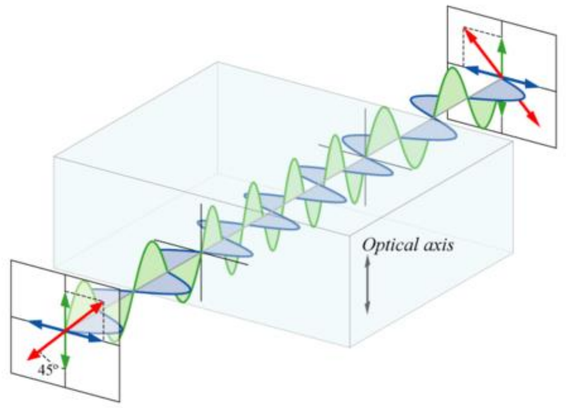

birifrangent material that shifts the polarization direction of linearly polarized light of 2θ

θ is the angle between polarization vector and vertical direction

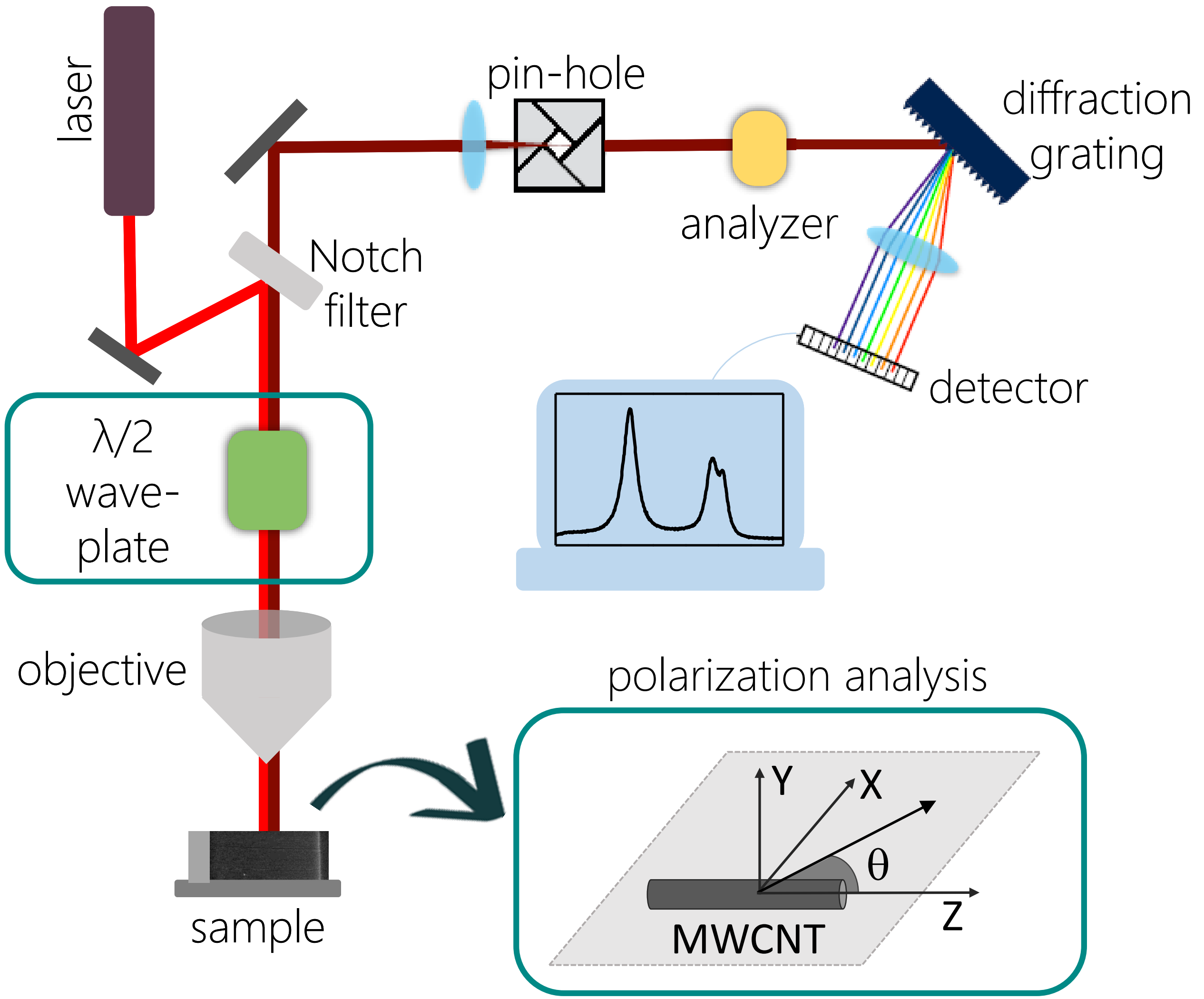

Polarization analysis

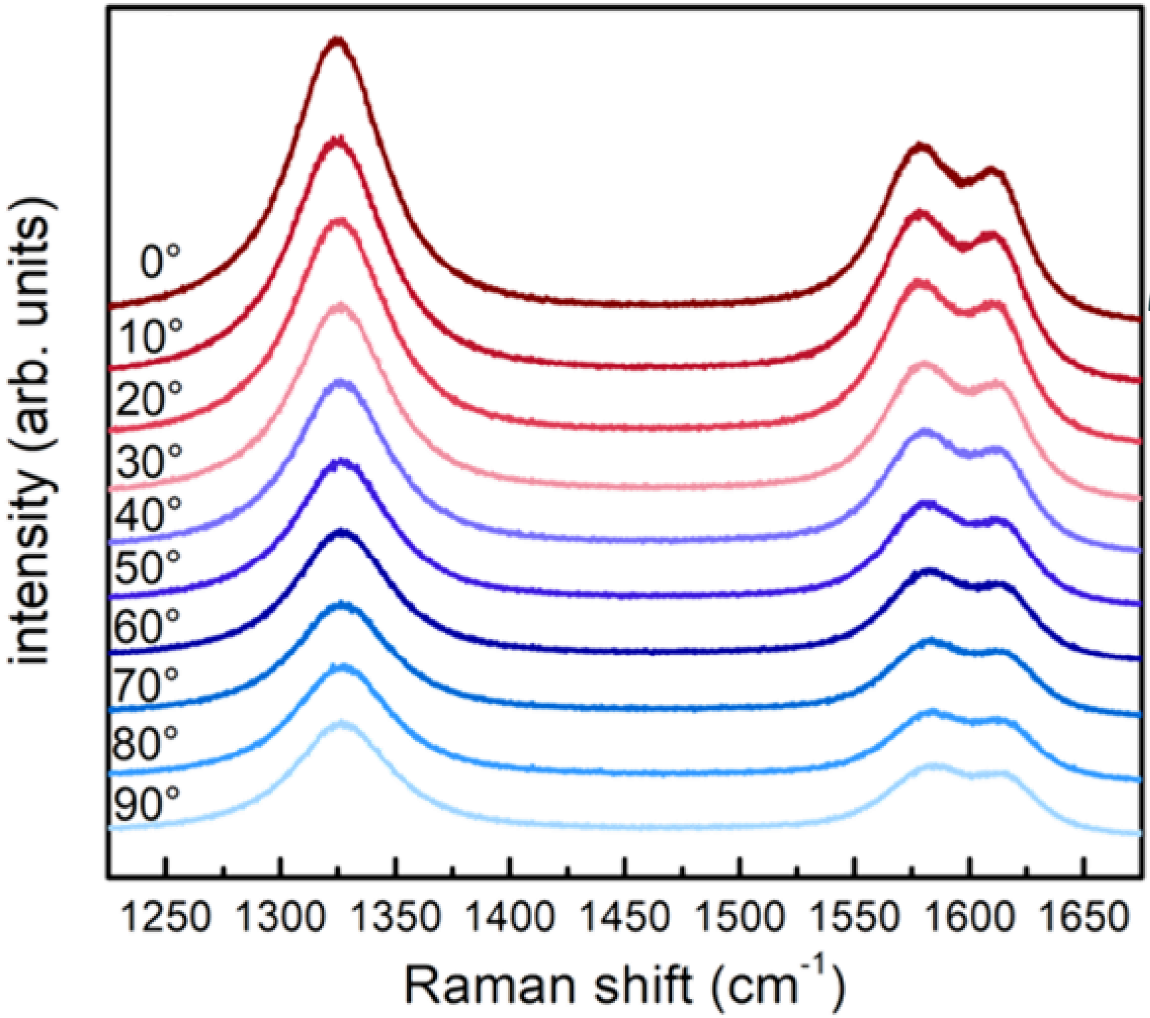

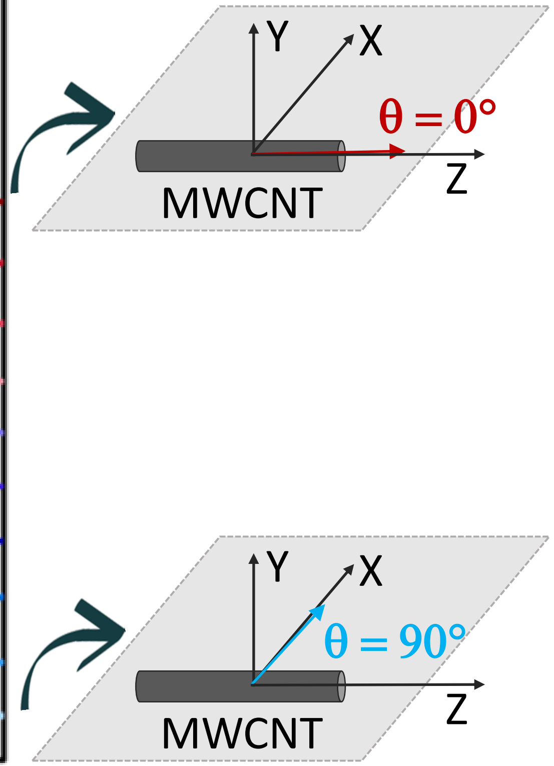

F. Ripanti, et al., under review in The Journal of Physical Chemistry C

Polarization analysis

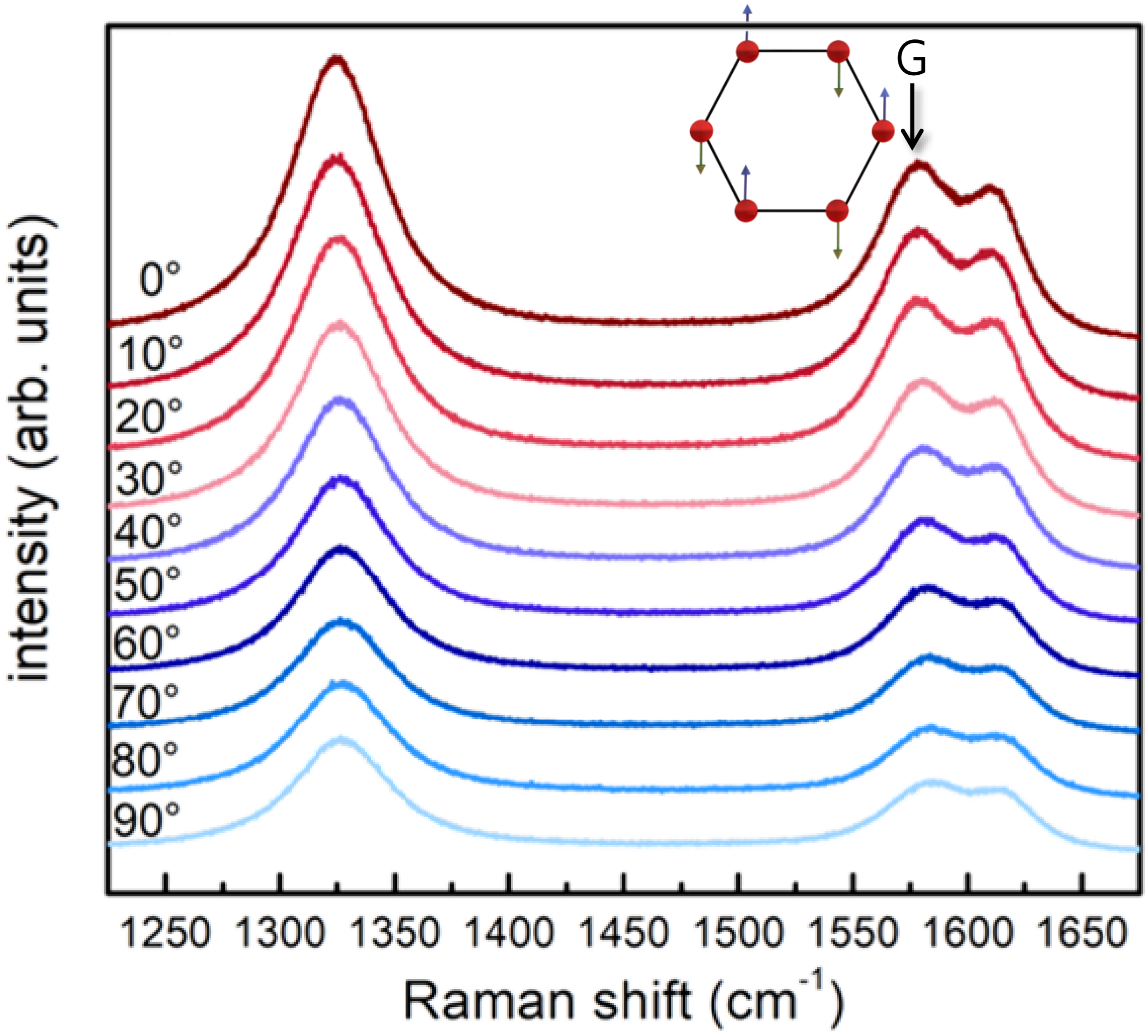

clear dependence of the Raman intensity on the polarization angle, confirming the high directional response of the sample

how can we explain this behavior?

- G-peak intensity as a function of θ
- **Raman tensor** for the corresponding vibrational mode
- standard Raman selection rules

F. Ripanti, et al., under review in The Journal of Physical Chemistry C

Polarization analysis

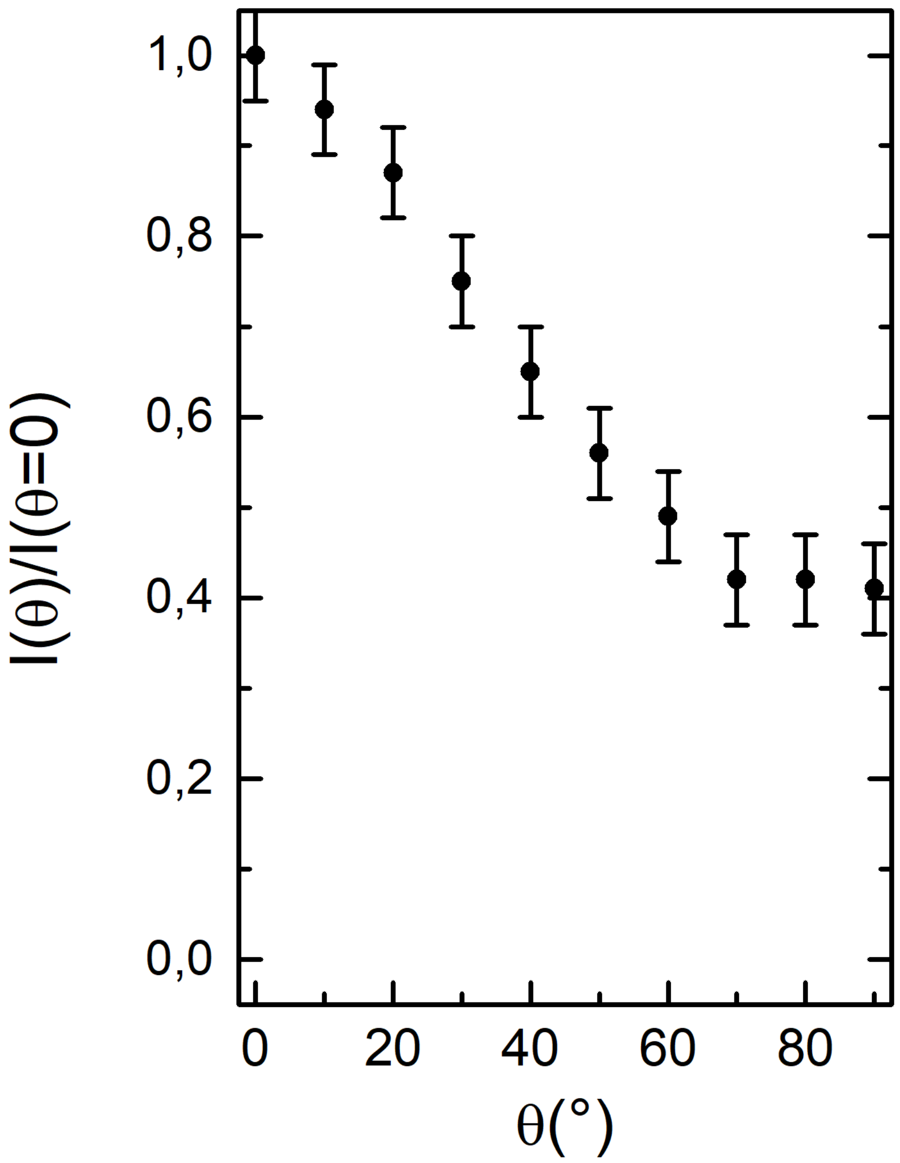

Polarization analysis

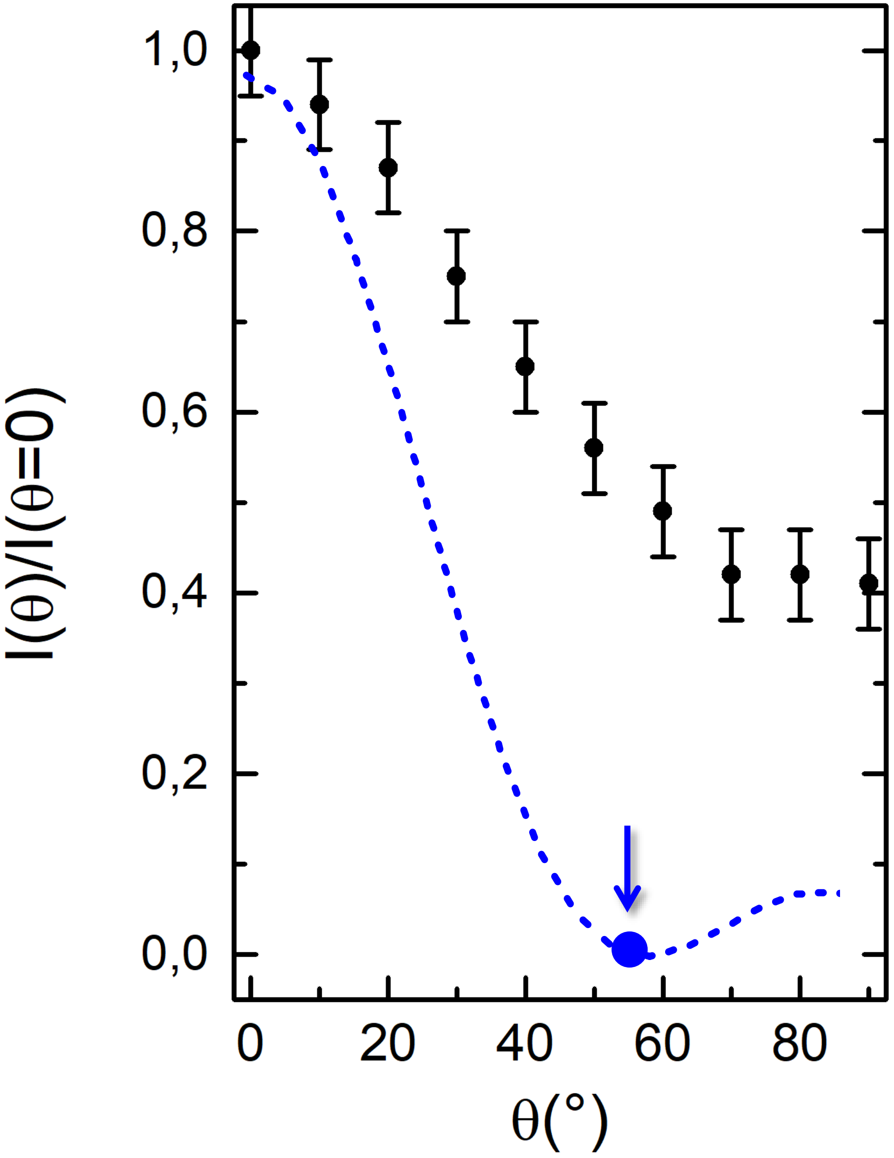

from Raman standard theory

$$I \propto |\varepsilon_i \cdot R \cdot \varepsilon_s|^2$$

$$R \propto \begin{pmatrix} -1/2 & 0 & 0 \\ 0 & -1/2 & 0 \\ 0 & 0 & 1 \end{pmatrix}$$

Raman tensor for G mode

$$\boldsymbol{\varepsilon_i} = \boldsymbol{\varepsilon_s} = \boldsymbol{\varepsilon} = \begin{pmatrix} sin\theta \\ 0 \\ cos\theta \end{pmatrix}$$

VV configuration

$$\frac{I^{VV}(\theta)}{I^{VV}(\theta = 0°)} = (cos^2(\theta) - \frac{1}{2} sin^2(\theta))^2 = \frac{1}{4}(3cos^2(\theta) - 1)^2$$

- minimum is reached for θ ~ 55°
- intensity minimum = 0

Polarization analysis

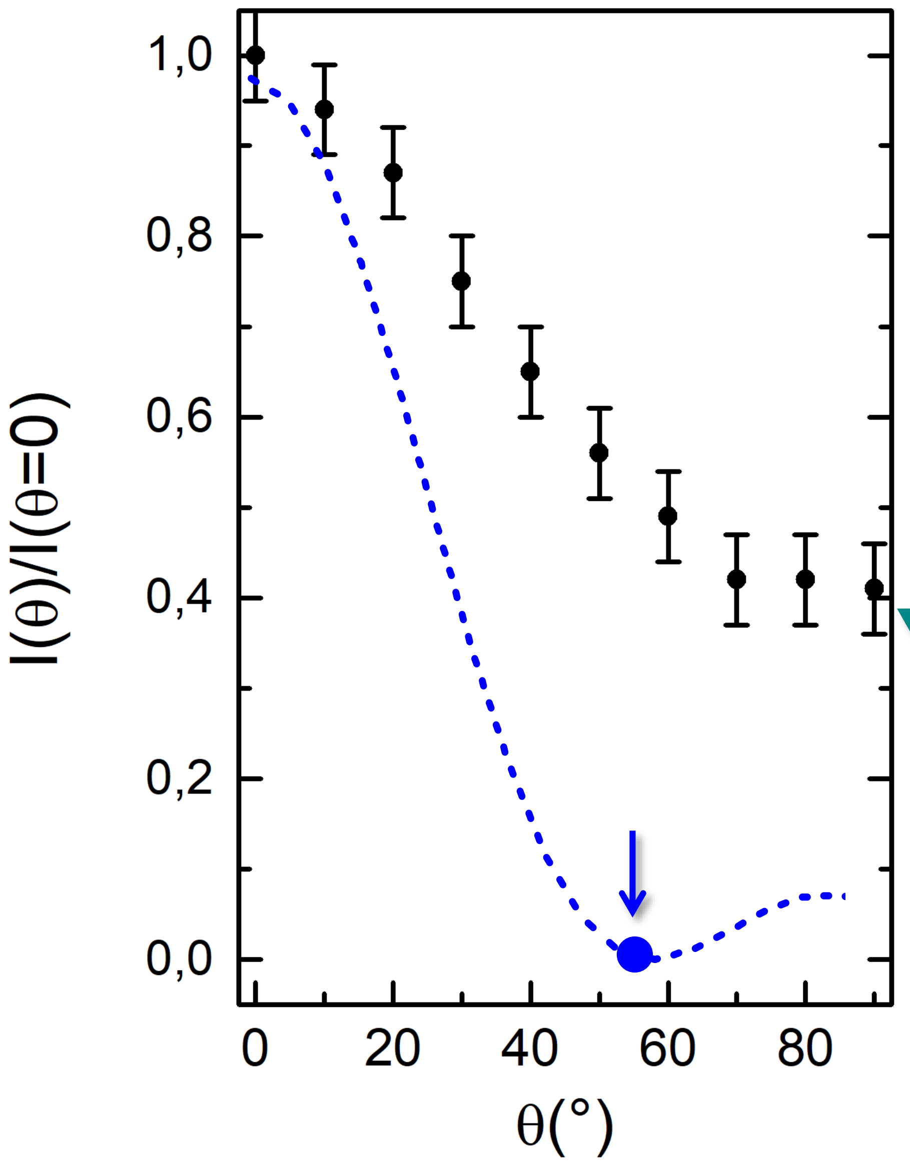

from Raman standard theory

$$I \propto |\varepsilon_i \cdot R \cdot \varepsilon_s|^2$$

$$R \propto \begin{pmatrix} -1/2 & 0 & 0 \\ 0 & -1/2 & 0 \\ 0 & 0 & 1 \end{pmatrix}$$

Raman tensor for G mode

$$\boldsymbol{\varepsilon}_i = \boldsymbol{\varepsilon}_s = \boldsymbol{\varepsilon} = \begin{pmatrix} sin\theta \\ 0 \\ cos\theta \end{pmatrix}$$

VV configuration

$$\frac{I^{VV}(\theta)}{I^{VV}(\theta = 0°)} = (cos^2(\theta) - \frac{1}{2} sin^2(\theta))^2 = \frac{1}{4}(3cos^2(\theta) - 1)^2$$

our results:

- minimum is reached for **θ ~ 90°** (polarization vector perpendicular to the CNT axis)
- the intensity **minimum does not reach zero** value

- minimum is reached for θ ~ 55°
- intensity minimum = 0

Polarization analysis

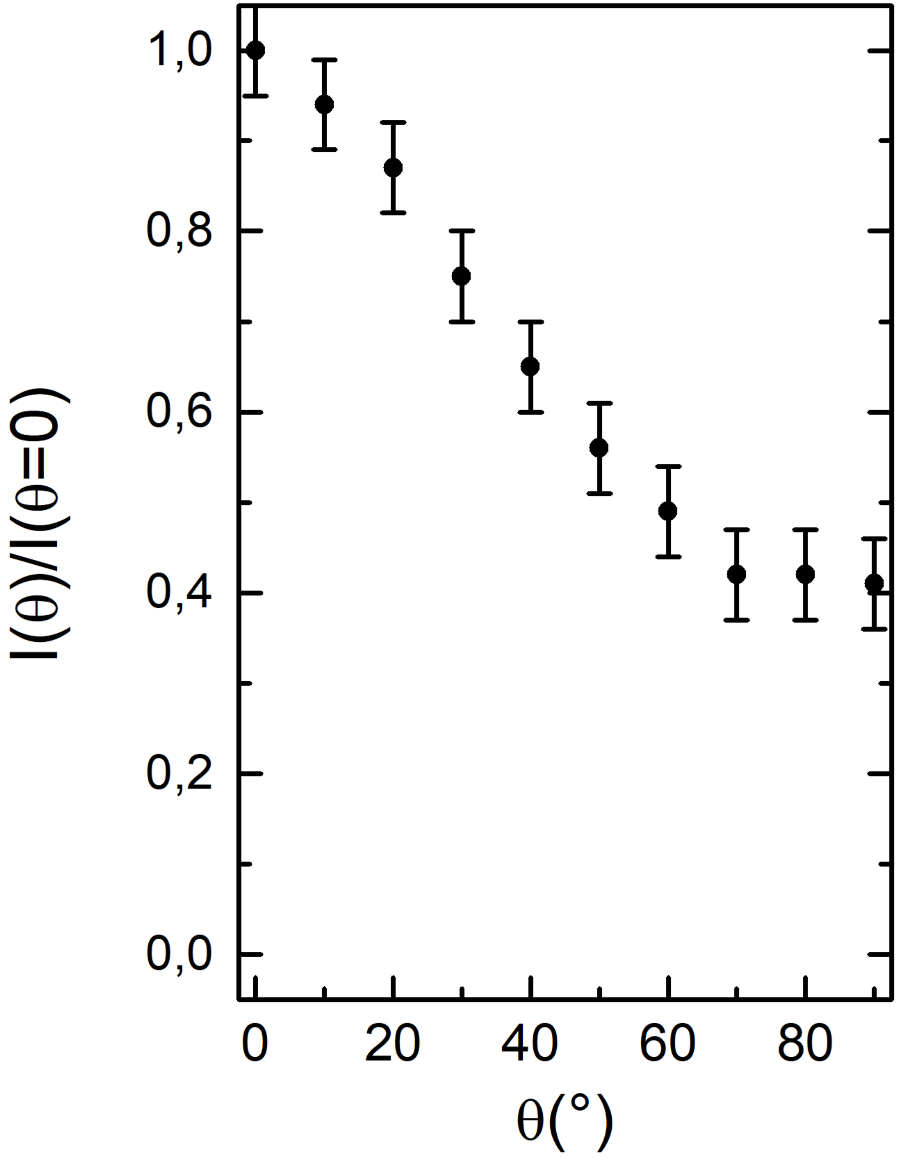

a new different approach:

fitting parameter

$$I^{VV}(\theta)|_{\exp} = \int [cos^2(\theta') - \frac{1}{2} sin^2(\theta')]^2 * \frac{1}{\sqrt{2\pi\sigma^2}} e^{-\frac{(\theta'-\theta)^2}{2\sigma^2}} d\theta'$$

theoretical function

g(θ′-θ)
gaussian angular distribution

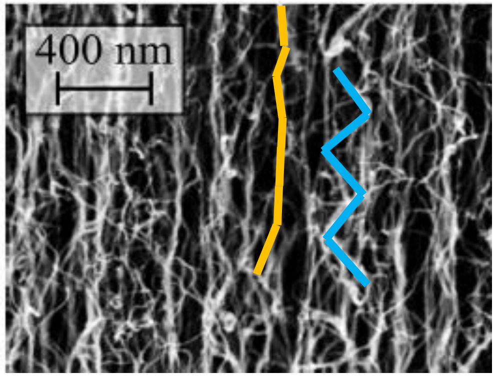

F. Ripanti, et al., under review in The Journal of Physical Chemistry C

Polarization analysis

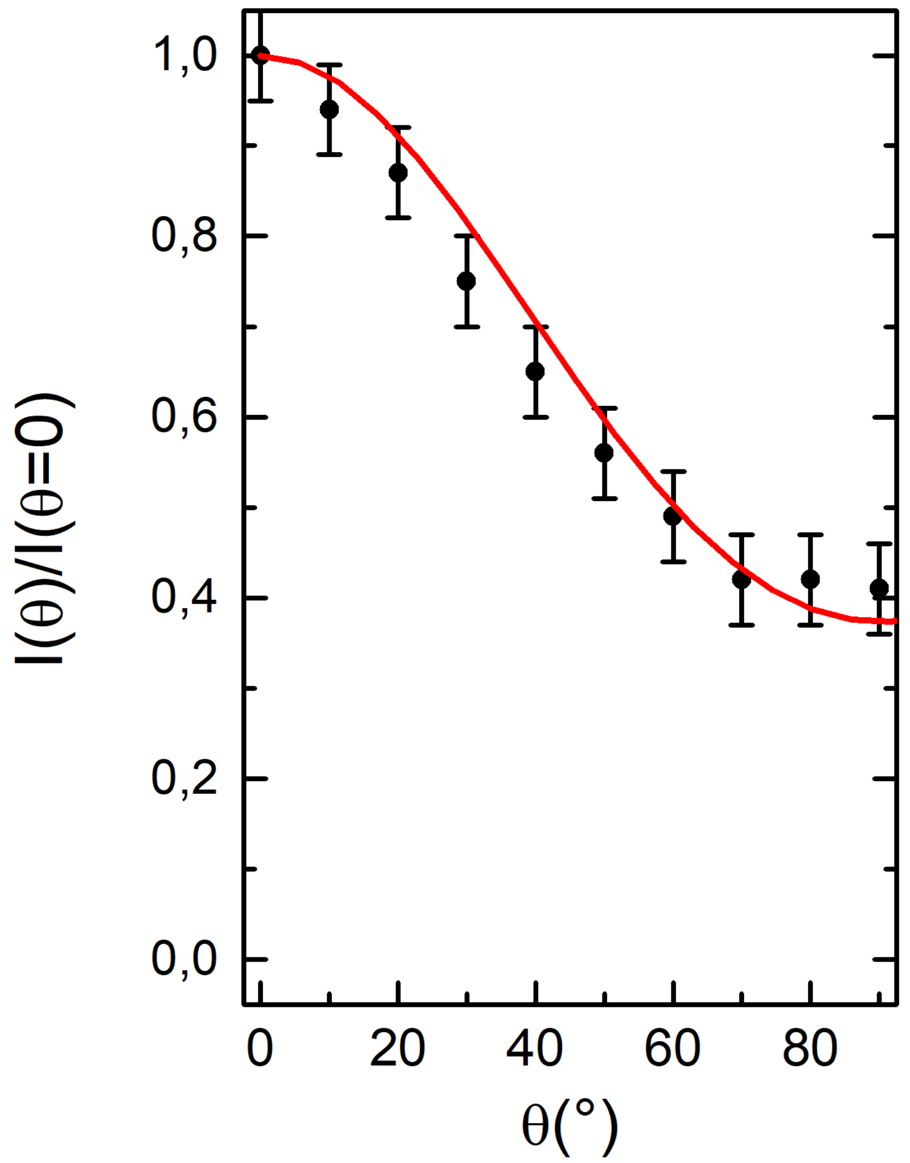

a new different approach:

$$I^{VV}(\theta)|_{exp} = \int [cos^2(\theta') - \frac{1}{2} sin^2(\theta')]^2 * \frac{1}{\sqrt{2\pi\sigma^2}} e^{-\frac{(\theta'-\theta)^2}{2\sigma^2}} d\theta'$$

fitting parameter

theoretical function

g(θ′-θ)
gaussian angular distribution

σ is the only parameter, representing an estimate of the nanotube axis angular deviation from the vertical direction

best value: σ = 37°± 4°

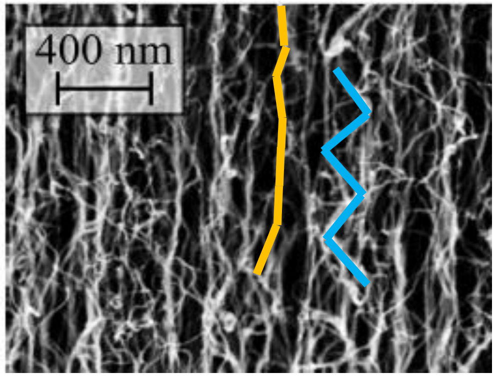

F. Ripanti, et al., under review in The Journal of Physical Chemistry C

Conclusions

aim: study of the **directional** bombardment of CNTs

- CNT array is a highly anisotropic system
- Ar^+ ion bombardment at different angles
- XPS and Raman spectroscopy to demonstrate the directional effects

✓ preferential ion channeling parallel to the tube axis
✓ possible critical angle above 40°?

- CNTs are not highly aligned on the nanometric scale
- presence of columnar voids among bundles
- general method to quantify the local misalignment

✓ channeling in the bundle interstices?

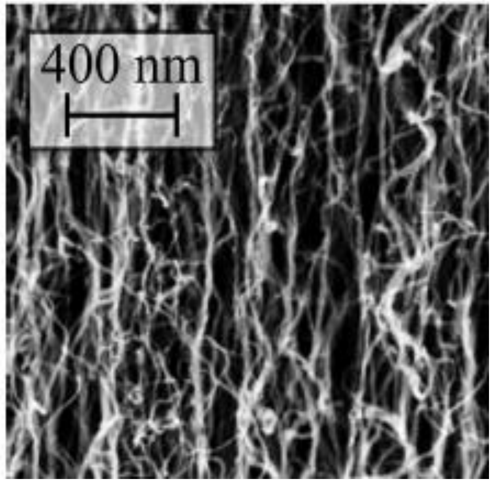

Acknowledgements

HPS group, Sapienza University
P. Postorino

LoTus group, Sapienza University
M.G. Betti
C. Mariani
G. D'Acunto (now @Lund University)
G. Avvisati
I. Rago

CNIS Sapienza
F. Mura

Sapienza University and INFN
G. Cavoto
A. Polosa
F. Pandolfi
E. Bernabei

University of Mons
C. Bittencourt
M. Scardamaglia

...and you for your kind attention!

Carbon nanotubes: morphology and properties

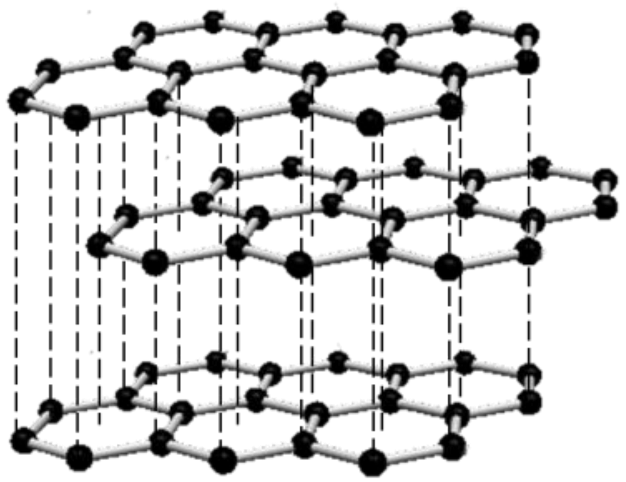

from graphite
to graphene…

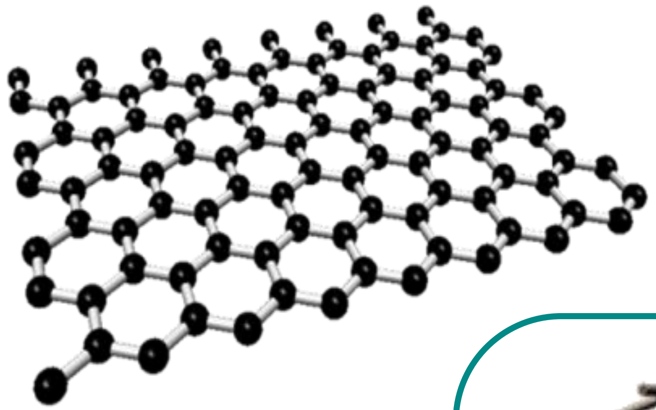

…wrapping a sheet of
graphene into a tube

single-wall carbon nanotubes
SWCNTs

multi-wall carbon nanotubes
MWCNTs

high anisotropy
quasi-1D materials

Ion bombardment: XPS and Raman spectroscopy

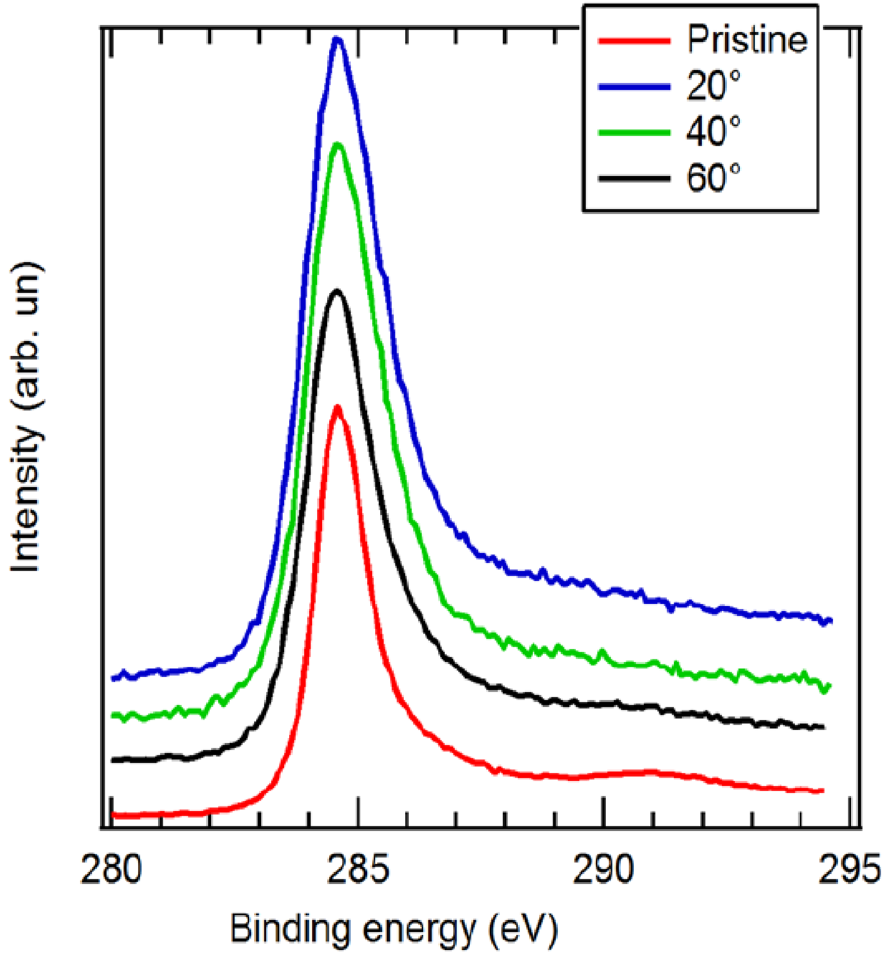

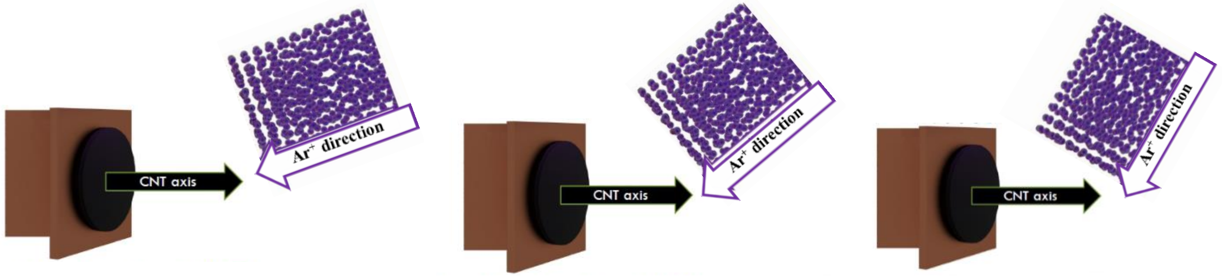

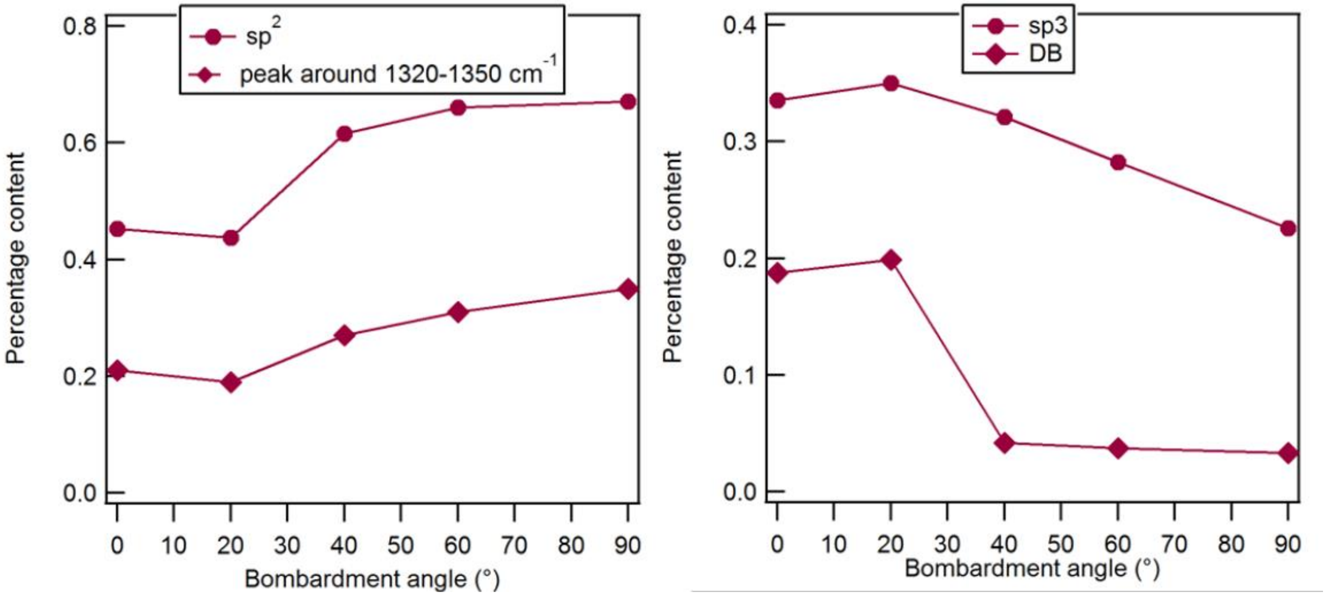

Francesca Ripanti
July 11, 2019

Ion bombardment: dose analysis

test method sensitivity: measurements at different ion bombardment energy (from 250 eV to 5 keV)

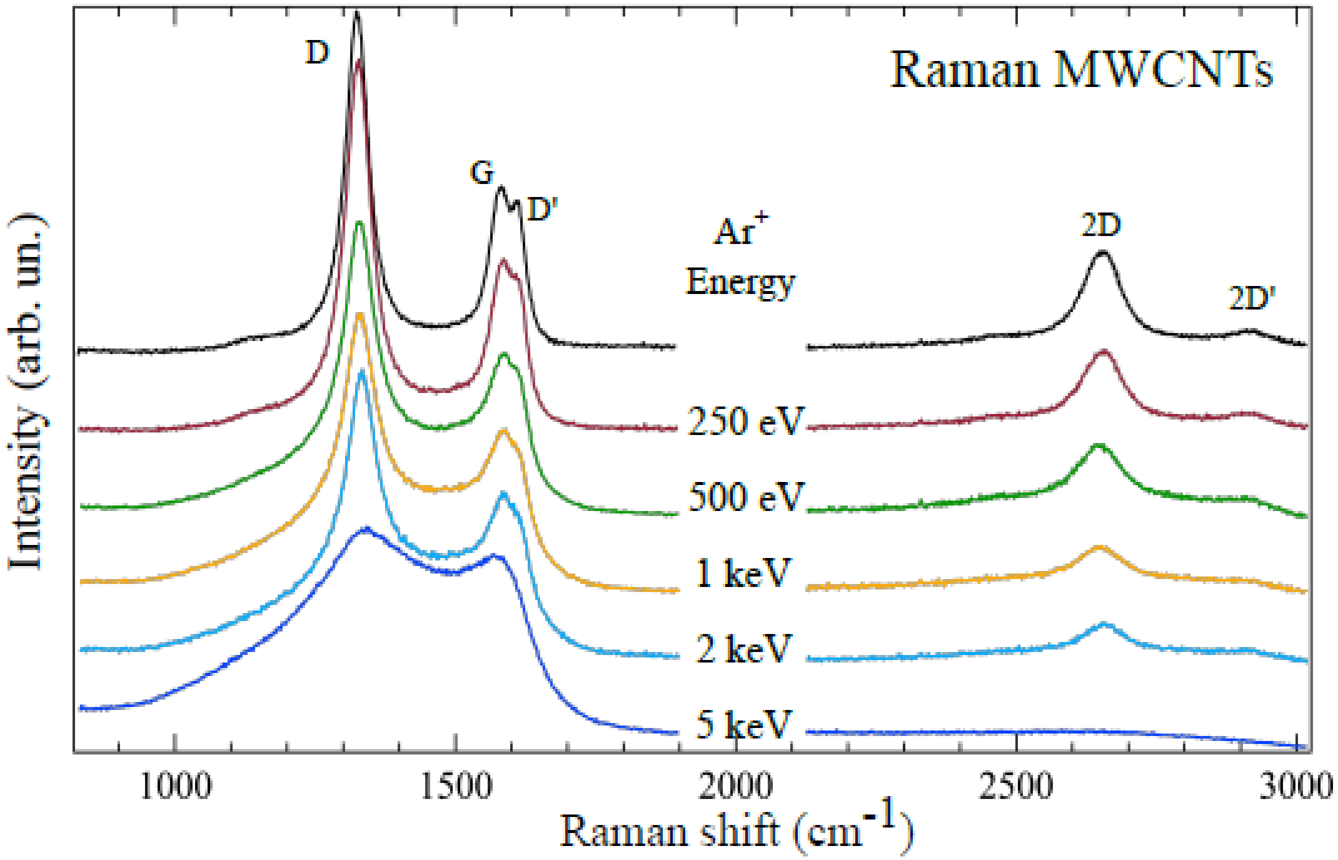

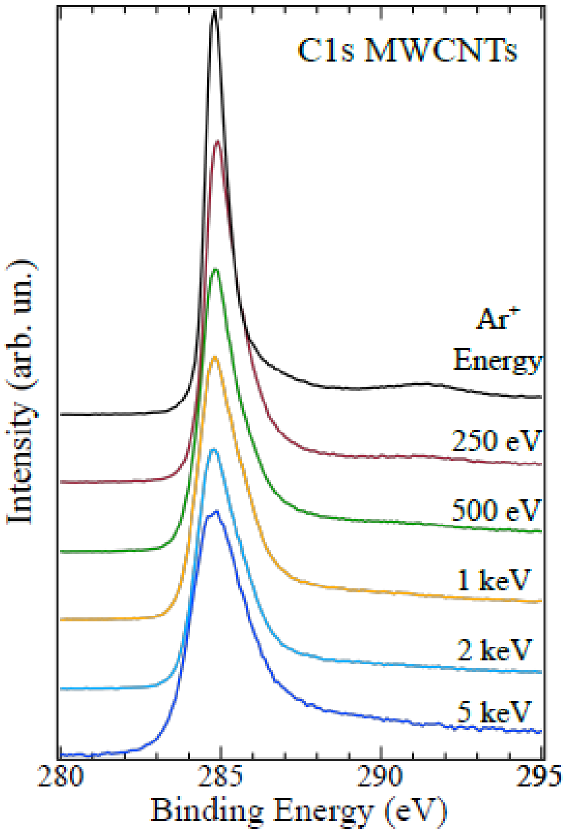

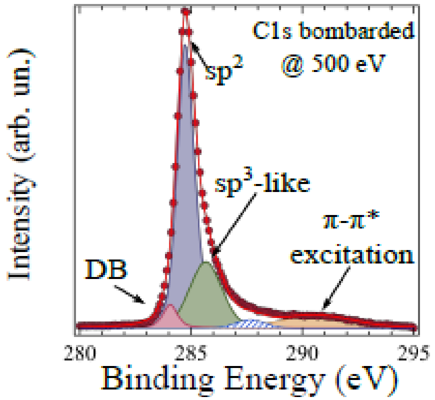

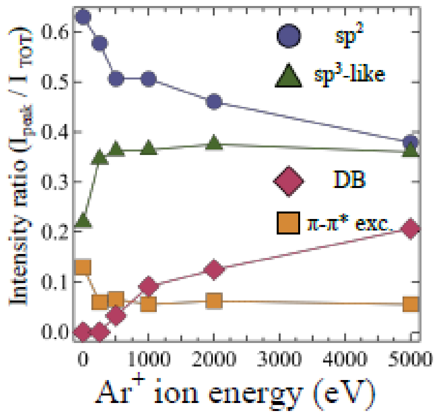

G. D'Acunto, F. Ripanti, et al., *Carbon 139, 768, 2018*

the amorphization depends on the energy of the bombardment ions:
- different Raman spectra for different energies;
- different XPS spectrum: analysis of the defect types as a function of the energy

Polarization analysis: comparison with literature

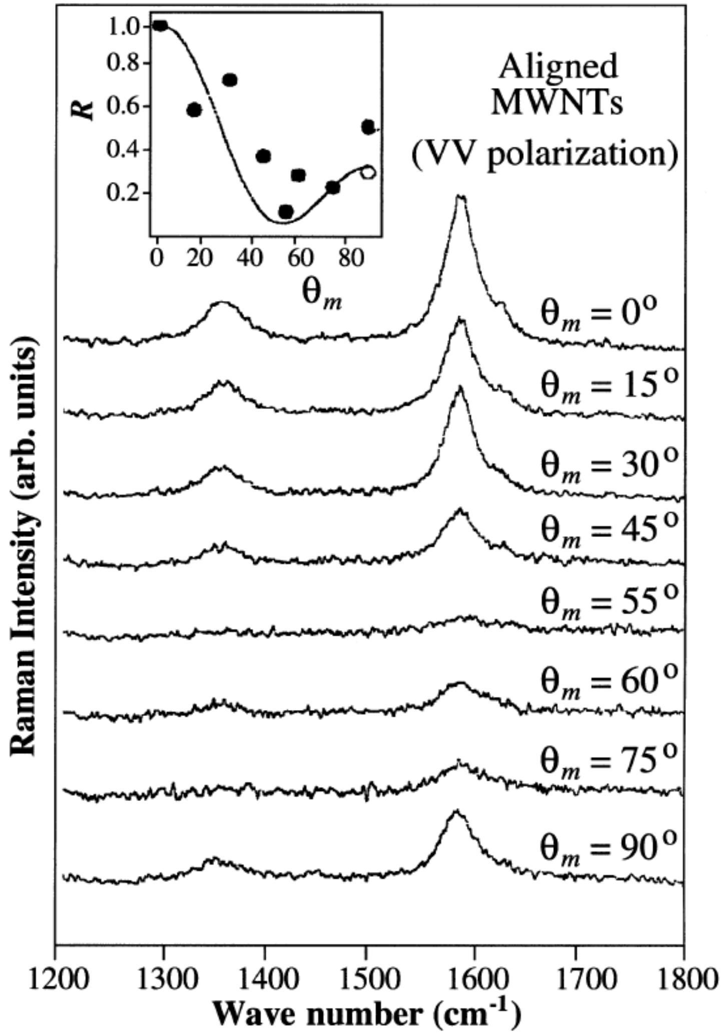

A.M. Rao et al., Physics Review Letters 84, 1820, 2000

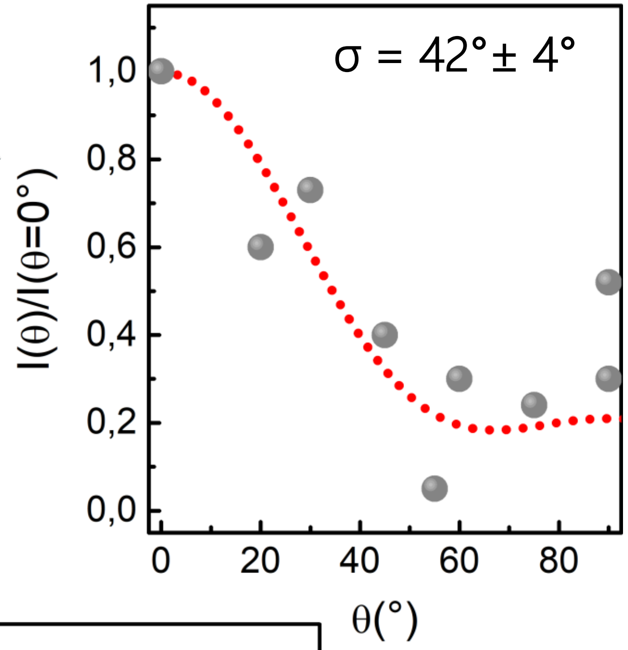

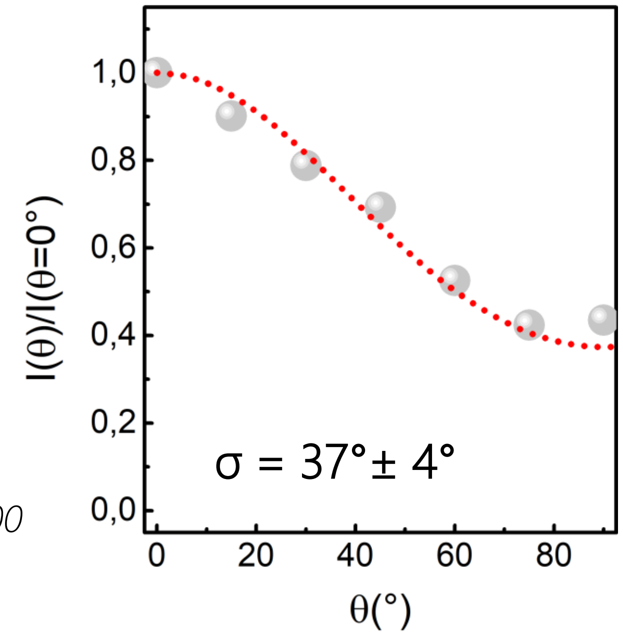

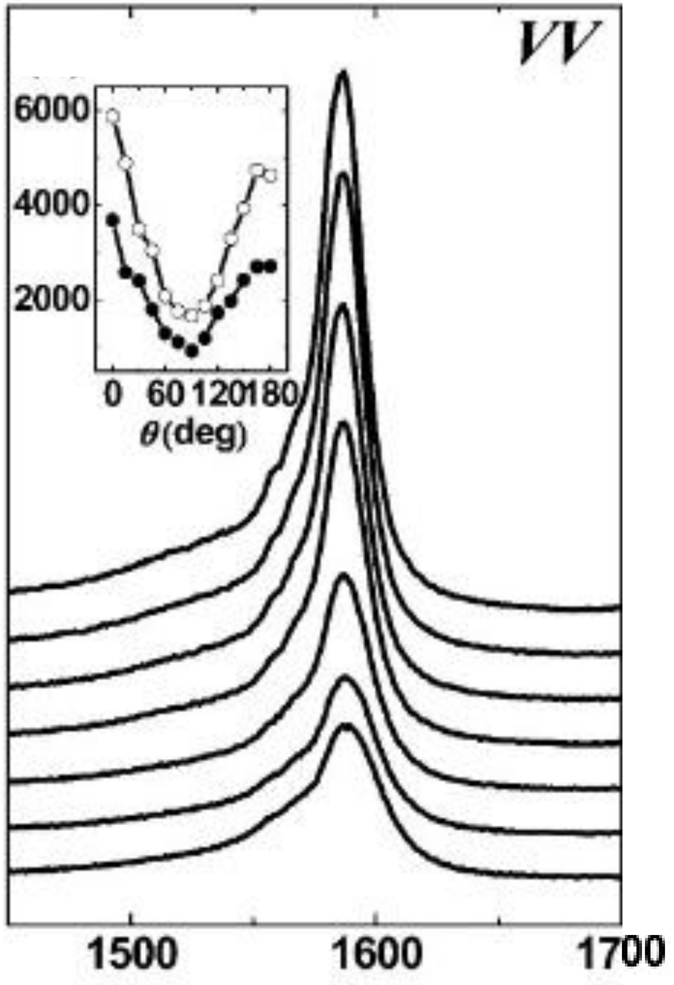

W. Ren et al., Physics Review B 71, 115428, 2005

Polarization analysis: close inspection of G-peak

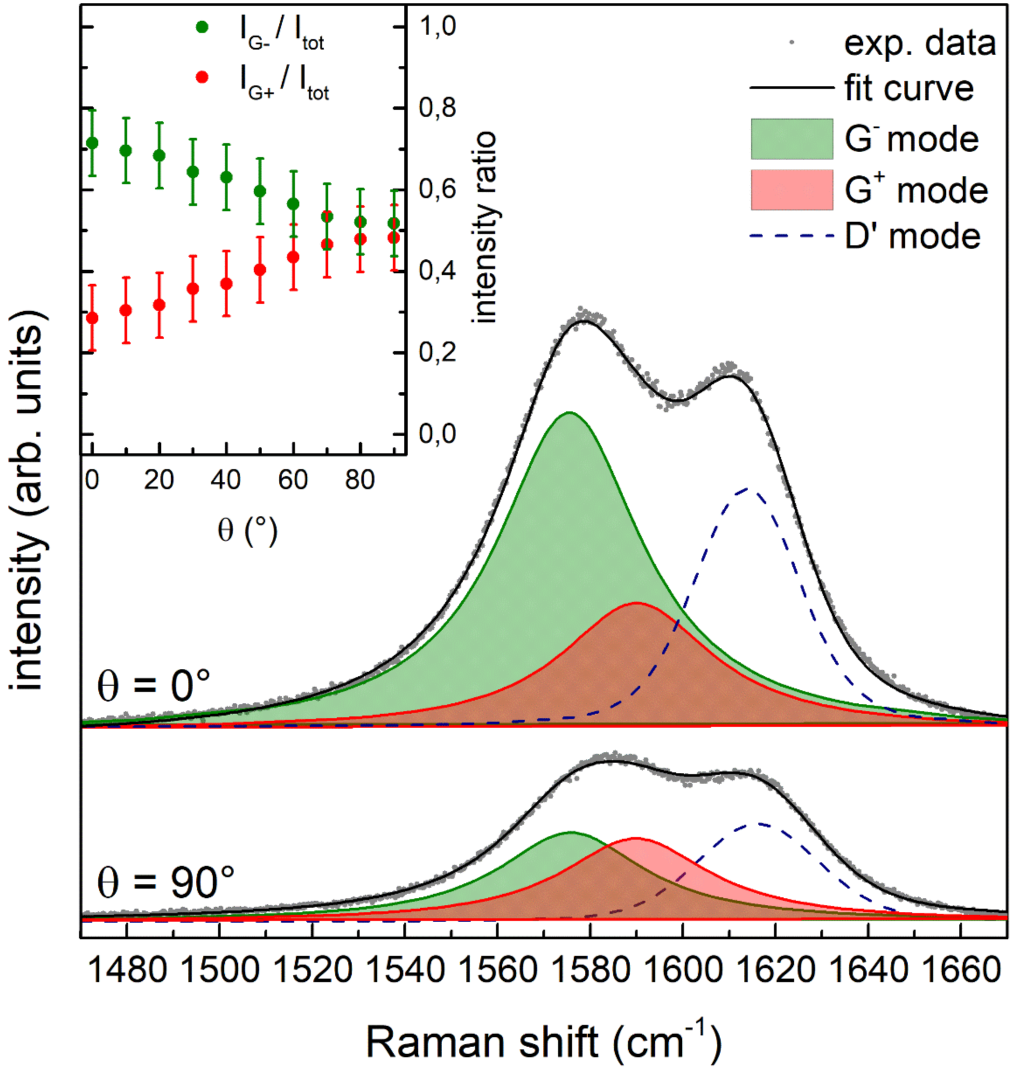

- spectral shape related to CNT nature (metallic/semiconductor)
- in metallic CNTs: G^- longitudinal mode
  G^+ transversal mode

↓

G^- (longitudinal):
maximum of intensity for $\theta = 0°$
(polarization parallel to CNT axis)

G^+ (transversal):
maximum of intensity for $\theta = 0°$
(polarization perpendicular to CNT axis)

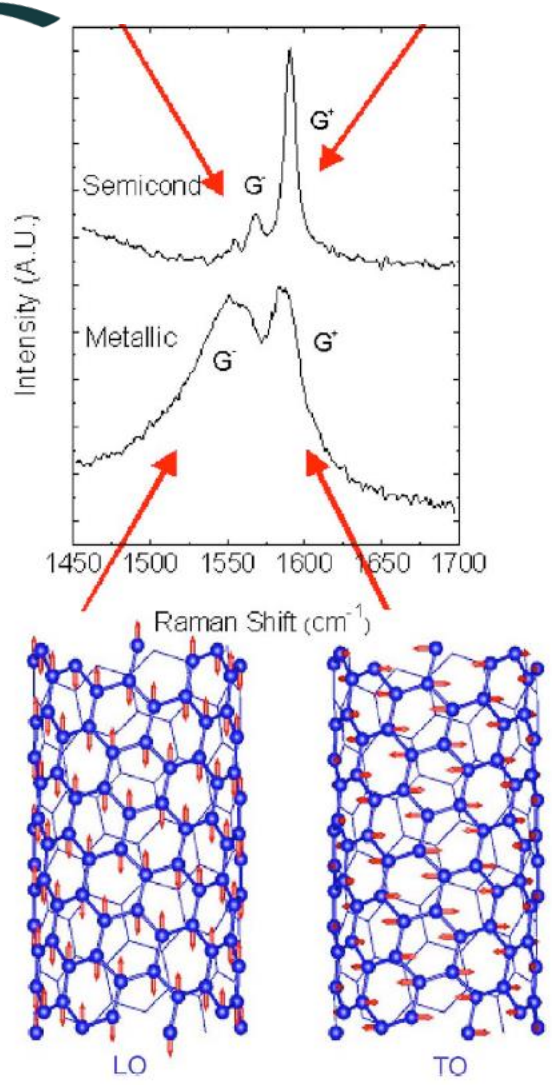

S. Piscanec et al., Physics Review B 75, 035427, 2007

F. Ripanti, et al., to be published in The Journal of Physical Chemistry C